# VECTORS IN PORPHYRY CU-AU EXPLORATION: ALTERATION AND METAL ZONING, COPPER CLIFF PROSPECT, MONTANA

By

Jeremy H. Fairbanks

Submitted in Partial Fulfillment
of the Requirements for the

Master of Science in Geology

New Mexico Institute of Mining and Technology
Department of Earth and Environmental Science

Socorro, New Mexico
May, 2009

# ABSTRACT

The Copper Cliff District of eastern Missoula County, Montana, is a small, inactive group of mines that produced copper and nominal amounts of silver and gold from the 1890's into the late 1940's. Historic production came from oxidized replacement ore associated with fault zones. The District came back into favor with large exploration companies in the late 1970's due to the recognition of quartz-alunite alteration in the District, which has been shown in other localities to be spatially associated with Cu-Mo-(Au) porphyry deposits. Since this recognition, exploration projects have been undertaken by Anaconda, Newmont, and Kennecott, the last of which began a deep drilling program on the property in 2006.

Because the target is a deeply-buried, Resolution-style deposit with little readily-visible surface expression, project leaders determined that the District would be a favorable location to test the effectiveness of using the SWIR PIMA™ spectrometer as an exploration tool to help define alteration zones and assemblages. The PIMA™, which can identify hydrated minerals in rocks with little sample preparation, was used to test over 1700 core, outcrop, and soil samples during the course of the project, establishing a representative distribution of points. To test whether the sampling program would be of use in focusing exploration efforts, this alteration mineralogy data was combined with surface and underground assays to assess the differences in metallic content among the various altered areas. Petrographic samples were collected to help characterize alteration assemblages, and

samples of alunite and pyrite were analyzed to determine their stable isotopic ratios of sulfur in an effort to understand the system's genesis.

This study concludes that at Copper Cliff the PIMA™ is of important albeit limited use, due to a number of factors such as the widespread occurrence of fine-grained, noise-producing sulfides, the inability of the instrument to distinguish between hypogene and supergene alteration minerals, and its inability to identify non-hydrated minerals that are important in some assemblages. Furthermore, the amount of data returned per sample is not sufficient to accurately characterize an alteration assemblage, and the instrument clearly cannot be used on its own to this end. However, the PIMA proved adept at recognizing certain important alteration minerals, namely alunite, and was used to create valuable distribution maps. Because of alunite's importance to exploration in the District, the PIMA™ has been shown to be an effective tool for exposing vectors to drilling sites.

Petrographic and isotopic work, as well as models of metal distributions within the Copper Cliff system, have shown that the porphyry developed from an Fe-rich, oxidized ore fluid. Mineralization above approximately 900 meters above sea level (ASL) took place at or below 200°C as evidenced by isotopic data, and was deposited by magmatic fluid interaction with meteoric water rather than magmatic vapor transport of metals. This accounts for the Au-poor nature of the near-surface mineralization as compared to other porphyry-related epithermal systems, the presence of alunite over a vertical span of 1000 meters, and the similar distribution of specular hematite. Robust conclusions concerning sulfide mineralization below 500 meters ASL require additional drilling, as sample density for these elevations is lacking, and current evidence suggests a significant change in mineralization below this level.

TABLE OF CONTENTS

LIST OF FIGURES

LIST OF TABLES

This thesis is accepted on behalf of the
Faculty of the Institute by the following committee:

_____

Advisor

_____

_____

_____

_____

_____

Date

I release this document to the New Mexico Institute of Mining and Technology.

_____

Student Signature Date

# 1. INTRODUCTION

Copper Cliff, a small mining district of the larger Garnet Range metals region, is a generally unproductive area relative to other nearby world-class districts such as Butte, Phillipsburg, and the Coeur d'Alene. Production was sporadic for almost 60 years before the complete cessation of active mining in the late 1940's, and it can be safely assumed that little money, if any, was ever made by the prospectors (Sahinen 1957). However, following Sillitoe's (1988) recognition that quartz-alunite alteration is often spatially and temporally associated with porphyry copper deposits at depth, and the concurrent discovery of this alteration type at Copper Cliff by Pederson (1988), the district has enjoyed an exploration renaissance. Exploration programs were undertaken by several major mining companies beginning in the 1980's, with large, world-class targets suddenly at the forefront.

A previous study by Anaconda geologists (Brannon et al. 1982) outlined the potential for high-grade mineralization in the realm of 400 million tons, with good values possible in copper, gold, and silver. Carbonate replacements, hydrothermal and fault breccias, and porphyry copper bodies were all outlined as targets by company geologists. Only replacement and breccia deposits were the targets of historic prospectors. However, the extensive faulting and alteration in the District makes extensions to the previously recognized resources possible, as well as boosting the likelihood of other deposits that have yet to be

discovered.

This study was undertaken with the help of Kennecott Exploration with the aim of using the presumably intact epithermal-to-porphyry transition zone as an analog to test methods of vectoring to the most promising drilling targets in similar terranes around the world. As mining targets become deeper and drilling costs increase, it becomes more and more important to be able to more confidently site drill holes. The large alteration footprint left by the emplacement of the intrusive stocks on the property creates an ideal laboratory to investigate how these alteration assemblages can be used as a quick and cheap avenue to this end.

## 1.1. Location and Physiography

Copper Cliff is located approximately 30 miles east of Missoula, Montana, in the Garnet Range between the drainages of the Clark Fork and Blackfoot Rivers (Figure 1.1). The Garnet Range highlands stand at an average of 5700 feet above sea level (ASL), with steep V-shaped valleys cutting between heavily-wooded mountain ridges. Copper Cliff itself is located on Union Creek, a tributary to the Blackfoot, on the northern edge of the range near the village of Potomac. While mining was historically important to the Garnet Range, today the dominant use of the land is logging for paper and lumber. Though this complicates access to the property, roads over public BLM lands access the Union Creek valley from the south via I-90. Access can also be had from the northwest through Potomac, although agreements with private landowners must be obtained in advance as ranches must be crossed. As the altered area encompasses 3/4 of a square mile (Brannon et al 1982; Ellsworth 1993), the ridges and tributary ravines around Union Creek were all part of this investigation.

Known concentrations of quartz-alunite alteration are present in the central "triple-point" of Union Creek (Figure 1.1., upper left). Only 8 patented claims exist on the property, though a large number of unpatented claims have also been staked both recently and historically.

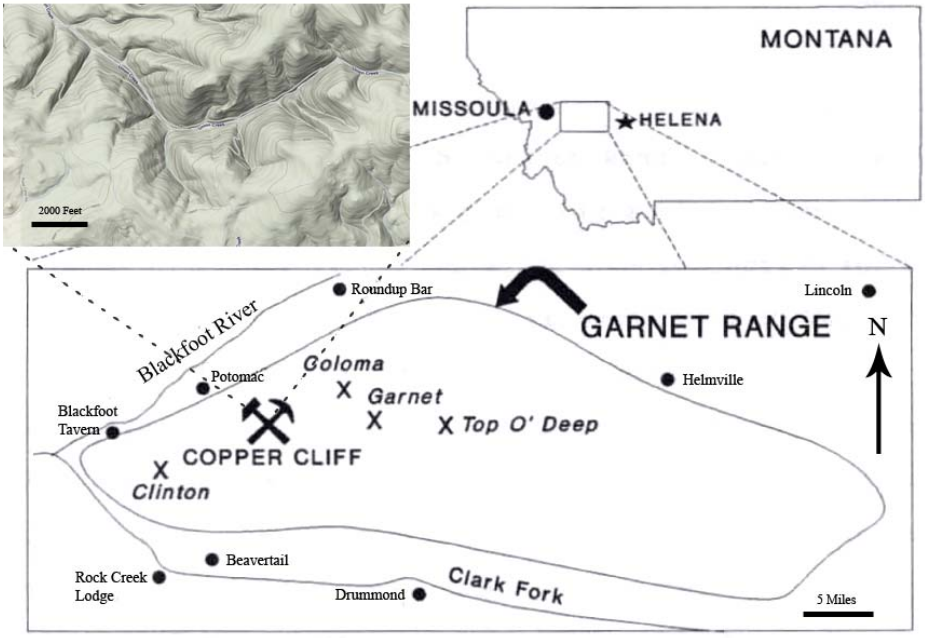


Figure 1.1. Location map of the Copper Cliff and surrounding Districts, including a 3D image of the area. Modified from Ellsworth (1993).

## 1.2. History of Copper Cliff

As Bannack, the first major gold discovery in Montana, began to play out, prospectors moved north and east in search of new sources of metal. This led to the discovery of large, persistent mining districts such a Butte, Virginia City, and Phillipsburg. One such major discovery was of placer gold at the mouth of Bear Creek in the Garnet Range, commonly known as Bearmouth. These placers yielded a large amount of gold; probably in the realm of $7,000,000 in the late 1800's (Pardee 1917). However, as these too were mined out, the search for the lodes in the interior of the Garnet Range began. This led to the discovery of several mining districts: Top o' Deep in 1866, Garnet in 1877,

| District | Au (t oz.) | Ag (t oz.) | Cu (lbs.) | Pb (lbs.) | Zn (lbs.) |
|---|---|---|---|---|---|
| Clinton | 212 | 31,744 | 226,545 | 36,642 | 3,200 |
| Coloma | 17,456 | 21,950 | 13,505 | 18,856 | 800 |
| Copper Cliff | 259 | 567 | 110,898 | - | - |
| Garnet | 113,139 | 101,962 | 166,699 | 7,442 | 1,744 |
| Blacktail | - | 6,487 | 1,300 | 1,336,170 | 26,700 |
| Top O' Deep | 2,575 | - | - | - | - |
| Totals | 133,641 | 162,740 | 518,945 | 1,399,110 | 32,444 |

Table 1.1. Production statistics for all the districts and mines of the western Garnet Range, including Copper Cliff. Modified from Ellsworth (1993).

Copper Cliff in 1891, Coloma in 1897, and finally Clinton in 1899 (Earll 1963; Irving 1963) (see Figure 1.1, bottom). The discovery of Copper Cliff by W. P. Shipler in 1891 caused a small amount of excitement at the time, due to the striking appearance of the 150-foot white cliff, visibly stained with large splashes of blue and green secondary copper minerals. The claims were purchased in 1900 by an English mining company, which did the largest amount of underground development on the property, amounting to some 1500 feet of shafts, crosscuts, and drifts at the Copper Cliff Mine. This was the largest development on the property, alongside the smaller Crescent, Tiger, and Leonard Mines (Pardee 1917). In all cases the targets were shallow, high-grade ores associated with hydrothermal breccias and replacement ores of Cu-Au-Ag (Brannon et al 1982). Both of these ore types are thought to have been misidentified as fault breccias at the time of extraction, though the collapse of the old workings precludes any underground assessment.

No information exists concerning the development and production from the Crescent and Tiger mines, and their former locations are in the realm of speculation. Of the remaining

two mines of the district, the Copper Cliff was by far more productive than the Leonard (Pardee 1917; Sahinen 1957). Though the bulk of production from the Copper Cliff occurred prior to 1916, sporadic smelter shipments into the later 1940's brought the totals for the district up to approximately $20,000 in copper, gold, and silver (Table 1.2).

| Year | Au (t oz.) | Ag (t oz.) | Cu (lbs.) | Value (in currency of the time) |
|---|---|---|---|---|
| 1891-1916 | 230 | 500 | 100,000 | $18,000 |
| 1917-1937 | - | - | - | - |
| 1938 | 14 | 31 | 3,888 | $891 |
| 1939 | - | - | - | - |
| 1940 | 5 | 14 | 1,310 | $333 |
| 1941 | 2 | - | 500 | $129 |
| 1942-1943 | - | - | - | - |
| 1944 | 6 | 7 | - | $215 |
| 1945 | 2 | 15 | 5200 | $691 |
| 1946-1960 | - | - | - | - |
| Totals | 259 | 567 | 110,898 | $20,259 |

Table 1.2. Summarized production from the Copper Cliff District during its lifetime. Modified from Earl (1963).

The Leonard, also called the Blue Bell as it was renamed in 1943, shipped some "21 carloads of [carbonate replacement] ore assaying 7 to 10 percent copper" (Sahinen 1957). Grades in the district were highly variable and difficult to predict, perhaps frustrating deeper and more profitable development efforts. Native copper nuggets the size of walnuts were common in the Copper Cliff Mine, including some reported to be the size of a man's head, and a large "boulder" of hydrothermal breccia was found in a fault zone that assayed 22% Cu. In 1910 the mine made its most storied shipment to the Tacoma smelter of 310 tons of ore that yielded approximately 77,000 pounds of copper (Sahinen 1957). However, most ore averaged 1% Cu and good material often had to be hand-sorted, a difficult task due to the nature of the rock and fine size of sulfides (Earll 1963; Pardee 1917). Large sums of money were spent chasing small, high-grade pockets with little success outside the main ore zone. According to Earll (1963), "any one of the several dumps represents the expenditure of more money than the value of the entire production of the district".

Since the discovery of Copper Cliff, the properties therein have changed hands multiple times as different individuals and small companies tried their hand at making a profit. The district was reopened for the last time in the 1940's, likely due to government incentives aimed at stockpiling metals important to the war effort, such as copper for ammunition. Major large-target exploration interest began in the 1970's with James Charlton and the American Mining Company (AMC), which did surface and geophysical work late in the decade. The property has also been leased by Cities Service Mining Company in 1977 (terminated work because of a drop in copper prices), Anaconda Minerals in 1980 (terminated work because they could not reach a lease agreement with the claim holders), Western Energy Corporation in 1985, Newmont Exploration Ltd. in 1991, and Kennecott Exploration in 2006 (Ellsworth 1993). Of these, only Newmont and Kennecott conducted extensive drilling programs, though with different targets; Newmont searched for shallow, bulk-mineable epithermal gold, while Kennecott is targeting a deep-seated, block-cave mineable porphyry Cu-Au ore body, similar to the Resolution discovery in Arizona. Anaconda's work produced some optimistic numbers for potential reserves for the deposit types found on the property, and an internal report touted the possibility of 340+ Mt Cu-Au porphyry ore at 1.0% Cu and 0.01 opt Au, 2.5+ Mt of hydrothermal breccia at 3.0% Cu, 1.0 opt Ag, and 0.1 opt Au, and 20+ Mt of carbonate replacement ore at 2.0% Cu, 1.0 opt Ag, and 0.1 opt Au (Brannon et al 1982).

### 1.3. Study Objective

Ellsworth's (1993) thesis was a collation of a large data package from Newmont Exploration, including geological, geochemical, and geophysical information. From this, he

determined the qualitative probability that the system was host to a porphyry copper body at depth, a conclusion that other, earlier researchers had speculated (Pederson 1988). Recognition of such a system from surface exposures is done with assays taken on soil, rock, and stream sediment samples, along with IP, gravity, magnetic surveys, and detailed geologic mapping. Drilling is done to verify the existence of a system and quantify its grade, and often must be done to depths of over 1500 meters; an expensive undertaking. In the past, surface assays of soil and outcrops have been the strongest determiners of where to site drill holes, but often due to hidden, post-mineralization structures, this is not always the best place to begin.

Given that drilling to such depths can cost in the realm of $500,000, any vectors that point to the best potential discovery hole should be investigated. The objective of this study is to use short-wave infrared (SWIR) spectroscopy to identify clay minerals, and hence subtle alteration assemblages, to use in conjunction with more traditional assay and mapping techniques. This may highlight new mineral zonations that can be used to better site drilling and save money on exploration, translating to more holes and a more fruitful project. In this study, surface zonation of metals and clays are compared with known assay data from the drill holes in order to "ground-truth" the picking of the best drilling sites. In addition, 3-dimensional models of metals in the known system are created for analysis and illustration, alteration and mineralization are analyzed petrographically, and important alteration minerals are tested for stable isotope ratios, in order supplement the findings. This approach will test the usefulness of SWIR spectroscopy in locating drill holes on prospects with porphyry copper targets similar to that of Copper Cliff, as well as give a useful characterization of the deposit valuable to future exploration in the District.

## 1.4. Methods

As the basis for this project was in large part a sizable data package obtained from Kennecott Exploration, a number of different people contributed to acquisition. Surface sampling for clay and chemical analysis was done mainly from 2006 to 2007 by myself and KEX Copper Group geologists Russ Franklin, Maarten de Moor, Scott Herman, Randy Boyer, Tim Worth, and Steve Beach. Rock samples were taken by grab, and documented with a detailed company sample card and GPS location. Soil samples were performed by traditional bulk sample methods, whereby 10-gallons of loose soil were dug from the B-horizon after clearing topsoil and removing biological material and rocks over 3 cm in diameter. Company sample cards and location information was also recorded for these samples. District-wide, 156 surface rock samples were obtained for clay mineral analysis and assay. Locations were determined mainly by ease of access due to the severe terrain, although several cross-valley transects were also done in July of 2007 to fill in gaps in the data. For the sake of time, soil analyses were confined mostly to ridges and valleys, due to the weight of each collected sample. 629 soil samples were taken for clay mineral analysis, and a further 258 for assay. This data was part of the KEX package.

Drill hole sampling was done concurrently with logging for all assays, which were sent for analysis at ALS Chemex in Elko, NV. For these, cut core was sampled, taking an even half of all cores. Samples for clay mineral study were taken every 2-5 meters on all cores and dried before analysis of the whole rock using a Spectral International Inc. (SII) PIMA™ SWIR field-portable spectrometer. The Spectral Geologist™ (TSG) software package was used to automatically analyze the spectra for each sample. Core was sampled a third time for the petrographic study. This sampling procedure was largely subjective, and was not

done at a regularly-spaced interval. Instead, samples of the best and most representative material were taken at intervals designed to be demonstrative of the distribution of alteration as recorded in the company core log. This included veins and alteration type contacts, as well as samples from the centers and edges of large, recognized sections of alteration in the holes. Samples were sent to Quality Thin Sections of Tuscon, AZ to be made into polished sections, and analysis of both reflected and transmitted light was done using a Nikon Optiphot-POL petrographic microscope. Three-dimensional interpolated underground computer models and maps were created using the RockWorks 2004™ software package, and surficial maps and displayed data were created in ESRI ArcGIS™. Sulfur isotopic data was collected by sample combustion in an EA and analyzed by using a Thermo-Finnigan stable isotope mass spectrometer in continuous flow mode.

## 1.5. Previous Investigations

The importance of alteration minerals in exploration and reconnaissance has been recognized ever since the categorization of gangue mineral assemblages, and is not unique to porphyry-type ore bodies. Every hydrothermal deposit type has its own signature assemblage and zonation pattern, and many researchers have recognized this uniqueness. Only a few examples of this work include the use of illite crystallinity in identifying thermal anomalies is rocks overlying hydrothermal Cu deposits (Duba and Williams-Jones 1983), illite crystallinity in phyllite as an indicator of underlying porphyry Cu mineralization (Jin et al 2002), and the use of clay composition and structure as an indicator of fluid temperature and chemistry in porphyry-associated alteration assemblages (Parry et al 2002).

Ground-based, field-portable methods are the most commonly used and studied ways

of both quantifying and qualifying alteration mineralogy at a prospect. Spectral International Inc. rents their PIMA™ spectrometers to mining and exploration companies on a monthly basis to meet the demand for such analyses. The use of these units is far cheaper, faster, and comparatively as accurate as using X-ray diffraction or SEM for identification. Speed is of importance because any mineral anomalies surrounding a metal deposit are likely to be far larger than the deposit itself, and a large number of samples must be taken in order to gain a useful surficial depiction of the altered area. With this in mind, many researchers have turned to using space-based and high-altitude spectrometers run by NASA such as ASTER (Advanced Spaceborne Thermal Emission and Reflection Radiometer) and AVIRIS (Airborne Visible/Infrared Imaging Spectrometer) which combine good resolution and multiple infrared bands with the ability to sample huge swaths of land in minutes. Laborious post-processing notwithstanding, this can be a powerful way to visualize clay mineral zonation on the surface, or locate the traces of hidden and buried deposits. AVIRIS, flown at an altitude of 20,000 meters, has even been used to accurately determine the composition of oxidized “leached caps”, and can take a swath 10.5 km in width with the capacity to store 1000 km worth of data (Berger et al 2003). Thus, a large amount of information can be collected in less time, using a smaller number of personnel. This technique has been used successfully at Red Mountain, Arizona (Berger et al 2003), Hillsboro, New Mexico (Verdel et al 2000), the Zagros Mountains, Iran (Mars and Rowan 2006), and at various other properties in Nevada, Chile, and Argentina.

However, the ASTER and AVIRIS currently function on a less-than-ideal resolution for some applications. For example, AVIRIS returns data with a pixel size of 20x20 meters, with only one mineral reported for each pixel. Though more information can be garnered

through post-processing of the data, it is clear that much will be lost. High-altitude data acquisition is clearly useful for locating new exploration opportunities, but ground-based techniques must come into play when more subtle structures and contacts may complicate interpretation of the data. Such use of the PIMA™ and similarly-constructed field spectrometers has been investigated as an exploration tool in Sonora, Mexico (Martinez et al 1999), Xinjiang, China (Yang et al 2005), and numerous other mines and prospects all over the world.

# 2. GEOLOGY, ALTERATION, AND MINERALIZATON

Both the regional and local geology of Copper Cliff and the Garnet Range in general is discussed in some depth in Pardee (1917), Irving (1963), Kauffman (1963), and Wallace, et al (1977). No additional geologic mapping was undertaken as part of this study, though detailed outcrop, alteration, and structural maps were made available as part of the Kennecott Exploration data package. In addition, mapping done by Anaconda and Newmont geologists and compiled in the thesis by Ellsworth (1993) supplemented this most recent work. Thus, the body of geologic maps and cross-sections available for the district is robust, and gives the researcher a clear insight into the regional and local stratigraphy and structure, as well as the intrusive and volcanic histories. Information on the alteration and mineralization of Copper Cliff is dealt with in depth in Ellsworth's (1993) thesis, drawn from Anaconda and Newmont geologists' work as well as his own. However, before the beginning of Kennecott Exploration's program in 2006, no deep drilling into the then-hypothesized porphyry copper body had been performed. Additional information gained via petrographic study of these drill cores has been added to the previously-available data.

## 2.1. Regional Geology

The Copper Cliff District exhibits complex faulting, important to the understanding of

any underlying mineral deposits. This is the local expression of the District's close association with the Lewis and Clark Line, also known as the Montana Lineament (Hawe 1974), which extends from the Couer d'Alene District of northern Idaho southeast to as far as the Lake Basin fault zone near Billings, Montana (Harrison et al 1974). This extensive structural zone is characterized by steeply-inclined dip-slip, strike-slip, and oblique-slip movement, and is hypothesized to have been reactivated since original activity during Proterozoic time (Reynolds 1979; Vice 1989). The lineament is also known as a host for many world-class mineral deposits, such as the aforementioned Coeur d'Alene, Philipsburg, and Butte Districts, in addition to a huge number of smaller districts. Reactivation of the Lineament's structures may also have served as conduits for mineralizing fluids in said mineralized areas.

During the late Cretaceous, activity in the Cordilleran Thrust Belt is likely to have influenced the emplacement of many igneous intrusive bodies such as the Pioneer and Philipsburg Batholiths of southwestern Montana, the Boulder Batholith of Butte, and the Garnet Stock of Copper Cliff (Ellsworth 1993; Reynolds, 1991). These mostly large, sill-like intrusions were emplaced along active thrust faults below the Sapphire Allochthon of southwestern Montana. The very northern edge of the Sapphire Allochthon is exhibited as the Blackfoot and Bearmouth thrust faults, just 8 miles south of the Copper Cliff property, near Cramer Creek, where sediments of the Proterozoic Belt Supergroup are placed on top of those of the Cambrian Hasmark Dolomite (Sears et al 1989).

## 2.2 District Geology

The Copper Cliff District lies at the boundary between two structural areas; one

characterized by tightly-folded and faulted Proterozoic and Paleozoic rocks (to the south), and another by open folds and overthrusts in Proterozoic rocks (to the north) (Brannon et al 1982). The District itself is underlain by a broad SE-plunging anticline composed of the metasediments of the Belt Supergroup, which are unconformably overlain by Cambrian carbonates and shales (Figure 2.1). Belt Supergroup metasediments in the District consist of the McNamara Formation, located in the northern part of the district, overlain by the Garnet Range Formation, which makes up the bulk of rocks exposed on the surface. Both of these units consist of stratified and often cross-bedded quartzite with maroon or light green

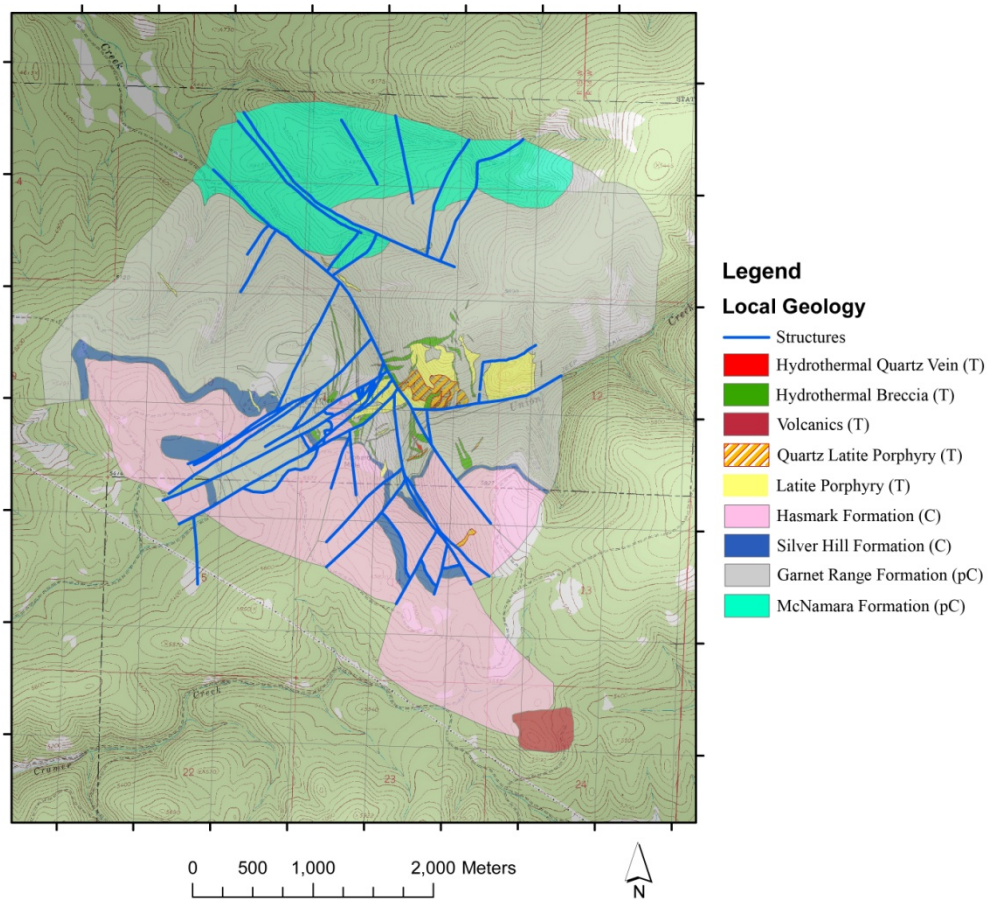


Figure 2.1. The product of Kennecott Exploration's ongoing mapping project in the Copper Cliff District. Hydrothermal breccias outcrop frequently in the District center, along with the intrusive stocks thought to have driven mineralization. The faults mined historically appear striking at approximately 50° in the center of the figure.

argillite, with the percentage of the former increasing as one moves stratigraphically upwards (Ellsworth 1993). This quartzite-dominated unit contacts the Cambrian Silver Hill Formation at an unconformity, although more recent mapping by Kennecott geologists supports a detachment fault as the cause of the missing strata (Franklin 2009, personal communication). The Silver Hill, consisting mostly of fissile shale with limestone interbeds, is normally underlain by the Flathead Quartzite, a marker bed familiar to Rocky Mountain

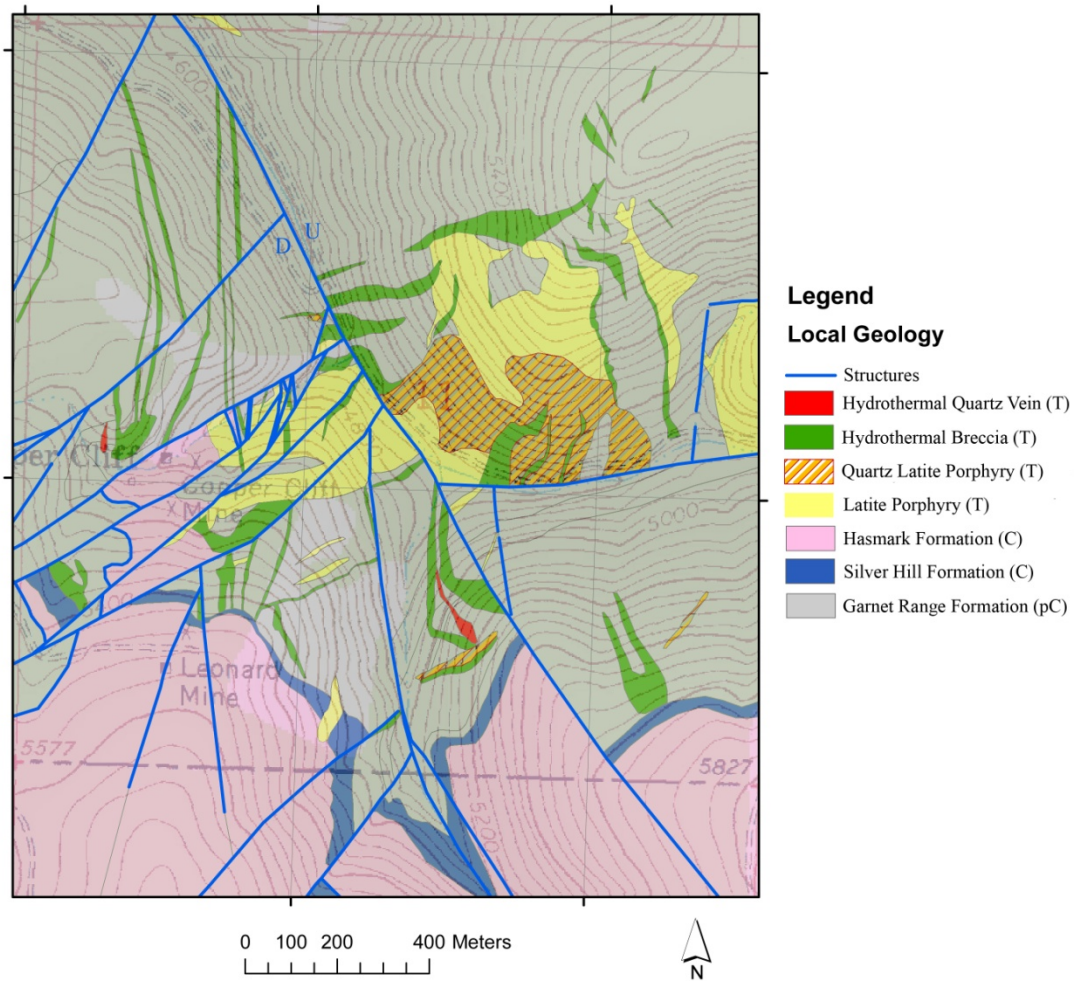


Figure 2.2. Detail of Kennecott Exploration's geologic map of the District, focused on the center of known mineralization. Breccias have multiple preferential orientations around the central intrusive body. The District's extensive structural deformation is complicated by limited fault exposures and heavy erosion. Fault locations are approximate in most cases. The relative movement along the important Union Creek Fault has been noted in this figure.

geologists. This is likely due to the location of the District on a topographic high during Flathead deposition. Above the Silver Hill Formation lies the Cambrian Hasmark Dolomite, a thick series of dark-gray, massive ridge-formers that normally marks the edge of the District and its main altered area, though jasperoids and weakly mineralized structures persist for some distance to the south. The Cambrian Red Lion Formation, exposed just south of the district, consists of nodular limestones with reddish-brown shales and siltstones.

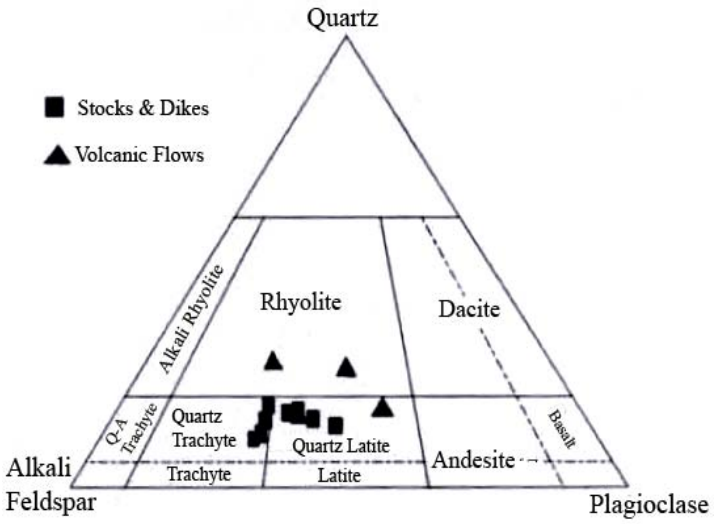


Figure 2.3. Ellsworth's (1993) Le Maitre classification of the Copper Cliff intrusives and extrusives, based on whole-rock geochemical analysis.

Stocks and hydrothermal breccia dikes of Tertiary age intrude both the Belt Supergroup and Cambrian sediments in the District, and are crudely aligned along ENE, NE, and NW trends, parallel with the regional deformation style of the Blackfoot series (Cox et al 1998; Mann and Sears 2004) (Figure 2.2). This group of igneous bodies is thought to be related to the mineralizing intrusives responsible for the Garnet and Coloma Districts' Au-Ag-Cu veins, and the Cu-Ag-Au-Pb veins of the Clinton District. Aeromagnetic data seem to suggest that they are connected at depth (Brannon et al 1982). Various sources have proposed a range of compositional terms for the intrusions at Copper Cliff, such as granite and andesite (Hawe 1974), granodiorite (Pardee 1917; Brannon et al 1982), quartz latite, and quartz trachyte (Ellsworth 1993; Brannon et al 1982). There may be several different intrusions of differing

compositions, but confusion also results from the extreme levels of alteration exhibited in most of the intrusions exposed at the surface. The distinction between quartz latite and andesite is determined via proportions of alkali feldspar, which can be added during alteration, and plagioclase, which can be altered and replaced. Additional petrographic work performed during Kennecott Exploration's drilling program supports Ellsworth's (1993) hypothesis that the composition of the majority of Copper Cliff's intrusions is quartz latite, though many show increased quantities of both plagioclase and silica, indicating a grading towards dacite. (Figure 2.3) Kennecott Exploration coined field terms for intrusives seen during drilling, resulting in most of these rocks being dubbed simply latite porphyry; they are labeled as such on geologic maps (Figures 2.1, 2.2).

Intrusions in the district consist of several small, cylindrical bodies collectively termed the Copper Cliff Plutons (Ellsworth 1993), and the much larger Union Hill Stock, which is purported to be the center of the mineralizing event for the District. All were emplaced during the early Eocene, approximately 56 Ma, and were followed by latite porphyry volcanic flows from 47.7 to 43.7 Ma. These flows can be seen capping Union Peak to the east of the district (Ellsworth 1993; Carter 1982) (Figure 2.1). While the Union Hill Stock and Copper Cliff Plutons have been dated at 56.4 +/- 1.5 Ma by K-Ar dating of unaltered biotite, alunite in altered rocks of the same intrusions are 48.4 +/- 1.3 Ma by the same method (Ellsworth 1993). Due to this temporal relationship, Ellsworth (1993) hypothesizes that the period of volcanism is the expression of a later intrusion at depth that provided the acidic fluids and gases required to form alunite in such great quantity.

The structural deformation of the Copper Cliff District is still not well understood, due mainly to the difficulty in locating and following faults under the advanced erosion and

heavy cover of the wooded slopes. During the District's short mining life, researchers such as Pardee (1917) noted that a clear understanding of the faults at Copper Cliff was of the utmost importance, since all of the highest-grade and most persistent ore bodies were associated with them. These large faults, named the Tiger, Leonard, Red Ore, and Black Ore faults by miners, strike roughly 50° azimuth but for the Leonard, and dip steeply to the NW and SE (Figure 2.1) (Sahinen 1957).

The exact nature of displacement on these faults is difficult to determine, but certainly includes a large amount of normal movement. The most striking structural feature is by far the large Union Creek Fault, the only structure on the property to trend in a NW direction, and the only one to parallel the Montana Lineament. Some 1500 feet of displacement along this large oblique-slip fault has juxtaposed deep and shallow parts of the Copper Cliff system together on opposite sides of Union Creek, through which the fault runs (Ellsworth 1993). Significantly, this considerable post-mineralization displacement has resulted in little or no difference in alteration styles across the fault. The Union Creek structure also complicates deep exploration in the area, as it is difficult to ascertain how far down the opposite side of any important mineralization has been dropped. Most faulting is attributed to the pre-ore Late Cretaceous Laramide Orogeny (Ellsworth 1993; Pardee 1917).

## 2.3. Mineralization

Copper Cliff, the original feature that drew prospectors to the area, was also originally the focus of mining activity in the District. However, it was quickly realized that this ore would only ever suffice as a flux agent for the smelters. Made up of heavily-silicified fragments of local quartzite, shale, and carbonate, in addition to some intrusive porphyry

clasts, the breccia bodies are tightly cemented (Pardee 1917). This extremely hard rock proved hardly worth mining, damaging tools and yielding little copper. Areas of over 2.5%-wt Cu are reported from quarrying efforts at the Cliff, with some even as high as 12%-wt Cu and 0.10 opt Au (Irving 1963; Weed and Gow 1919). However, other researchers since the days of active mining have concluded that an average of 1% for the entire breccia body would be optimistic (Sahinen 1957). A group of 14 channel samples collected by Johnson (1972) reported averages of 0.061 opt Au, 0.20 opt Ag, and 0.17% Cu. Efforts to mine the breccia body by underground stoping proved fruitless after it was found that the Cliff was truncated at shallow depth by a low-angle fault (Ellsworth 1993). The ore was also impossible to hand-cob, given the irregular distribution of sulfides. Enargite and famatinite are the two most common sulfide ore minerals, with pyrite as their usual gangue within the chalcedony matrix. Appreciable amounts of Cu-oxides were also found near the surface. Sulfide minerals are rarely visible to the naked eye, appearing as cloudy-gray patches encased in the amorphous silica of the breccia, even under a microscope. In a few high-grade pockets at the Cliff and other smaller, nearby breccia dikes, enargite can be recognized with the hand lens (Pardee 1917; Sahinen 1957). A sample collected at a prospect below the cliff showed abundant visible sulfosalts forming the matrix in a clast-supported hydrothermal breccia, and is likely to have contained 3-5% Cu.

The bulk of the material extracted at the mines of the District was taken from the underground workings that concentrated upon fault-related gouge and breccia, and oxidized/enriched replacement bodies. This ore was mined from the aforementioned steeply-dipping Red Ore, Black Ore, Tiger, and Leonard Faults, which hosted sections of rich ore in loosely-consolidated material in significant widths; over 50 feet wide in the case of the Red

Ore Fault (Pardee 1917; Hawe, 1974; Sahinen 1957). The Tiger, Leonard, and Red Ore Faults purportedly contained similar material, so named at the latter because of the red-yellow color of the highly-oxidized ore. This material was easily mined, and carried excellent copper values in the form of malachite, azurite, and chrysocollar. Flakes and marble-sized nuggets of native copper were also common in the stopes of this area, and one solid-copper boulder the size of a man's head is said to have been found (Sahinen 1957). The Black Ore Fault, by contrast, was only 10 feet at its widest, and was anomalously unoxidized, a characteristic that researchers have been unable to explain (Pardee 1917; Sahinen 1957). This ore zone was made up of gouge mix of finely-ground country rock and black sulfides, including pyrite, chalcocite, covellite, and enargite. The Red Ore is likely this same material, after oxidation (Ellsworth 1993). The Black Ore Fault is also the host for the pocket of 22%-wt Cu ore, the best grades ever found in the District (Pardee 1917). Other minor mineralization styles include some weak limestone replacements found in the Leonard mine, and some low-grade (0.011 opt Au) jasperoid dikes found in the Klenzie Mine (Ellsworth 1993; Childs and Mulholland 1988).

Other occurrences of Cu-bearing sulfides in the district were of course never exploited by early miners, being too deep and with little or no surface exposure, as well as far too low grade to be mined by the conventional underground methods of the time. Kennecott Exploration's drilling program has revealed a large fossil hydrothermal system. An acid-sulfate epithermal system occupies the District center, exhibiting enargite, famatinite, and pyrite within a silica and alunite matrix. Few sulfides besides fine disseminations and stringer veins of pyrite exist in this near-surface zone. In the realm of 500 meters ASL, below the center of the district, silica-lined veinlets and disseminations of pyrite,

chalcopyrite, molybdenite, bornite, and chalcocite are found. An anomalous 10 cm thick vein of solid chalcopyrite was also found in one hole. Sizeable intercepts of 0.5% to 0.8%-wt Cu are common below 500 meters ASL. The total extent of the system is unknown at the time of this writing, and work by Kennecott Exploration is ongoing.

## 2.4. Alteration

The Copper Cliff District exhibits a number of different alteration types, the recognition of which has evolved greatly over the last thirty years of study and exploration. Detailed mapping began in 1981, during Anaconda's examination of the prospect (Brannon et al 1982). Such maps were expanded and updated by Newmont in 1991, Ellsworth in 1993, and finally by Kennecott beginning in 2006. Until the deep-drilling program of the latter, alteration zones were only mapped as surficial features of the prospect. The present study has sought to expand the current knowledge base for Copper Cliff, and contributes new data significant to understanding the system.

Anaconda geologists mapped an altered area of over ¾ of a square mile, which they believed to be centered on the Union Hill Stock (Brannon et al 1982). The majority of rocks on the surface in this area are sediments of aforementioned Belt Supergroup, namely quartzite. These metasedimentary rocks were and are termed "bleached" due to their whiter color when compared to rocks of the same unit outside of the prospect. The field term has persisted, though analysis with the PIMA™ spectrometer has revealed these rocks to

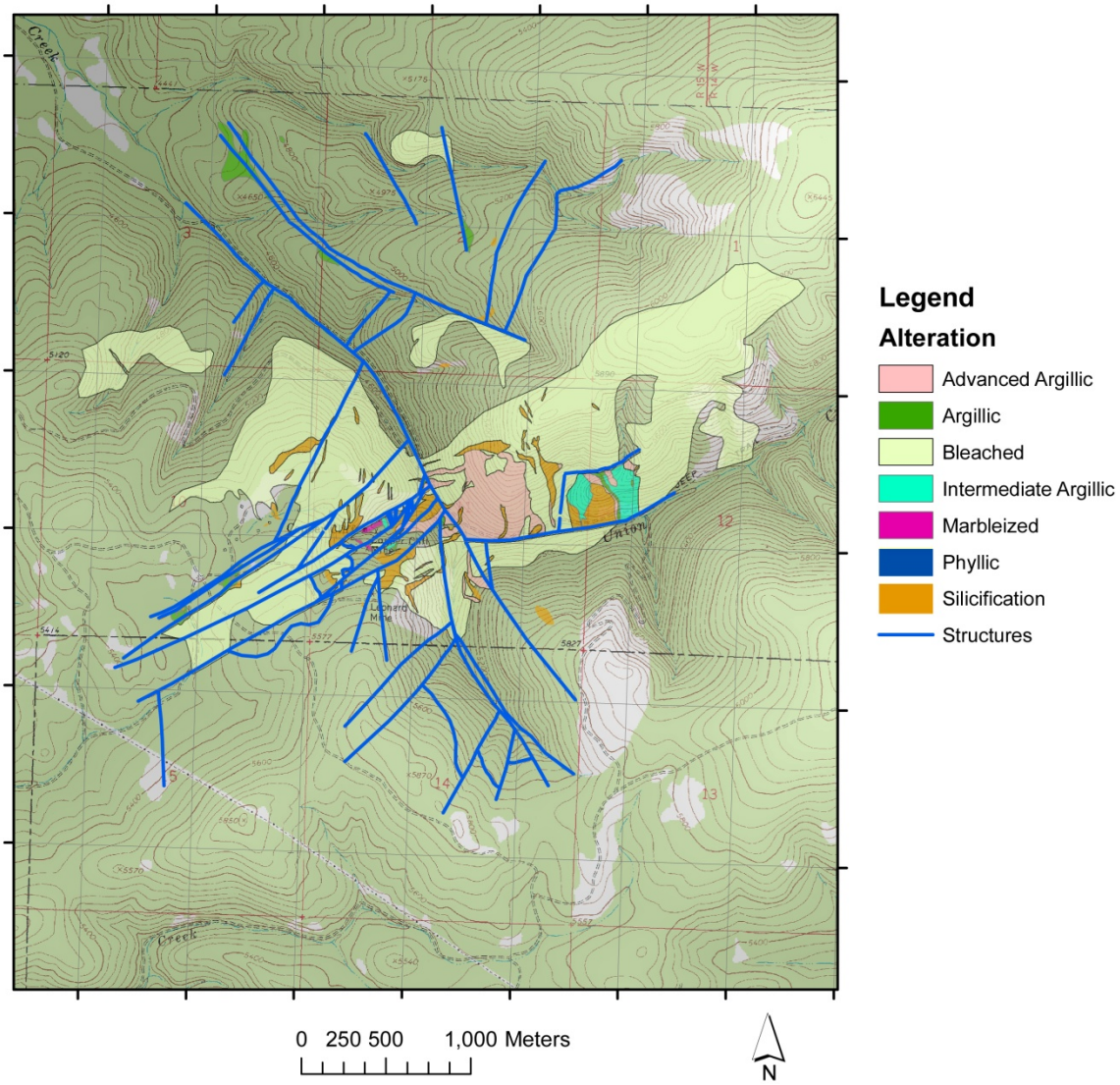


Figure 2.4. Kennecott's district-wide map of the alteration seen on the surface at Copper Cliff. Compared with the geologic maps presented in Figures 2.1 and 2.2, the similarities between the two are easy to ascertain.

have gained their white color from a moderate sericitization, something that Anaconda geologists surmised (Brannon et al 1982). Iron oxide liesegang weathering patterns are common throughout the district, and are likely the product of the weathering of the weak, pervasive pyritization of the country rock. Pyritization is more pronounced in and around the phyllic-altered breccia dikes, which are common around the center of the District, being the only units that form any sort of substantial outcrop. Along with phyllic alteration, the

hydrothermal breccia dikes and the surrounding rocks have been heavily silicified, often so much that original clast composition is difficult to discern. For instance, early intrusive units have in places become so flooded with silica that they bear all the characteristics of quartzite, and were often mistakenly mapped as such by experienced geologists. Some jarosite can also be found in breccias near the center of the District (Brannon et al 1982).

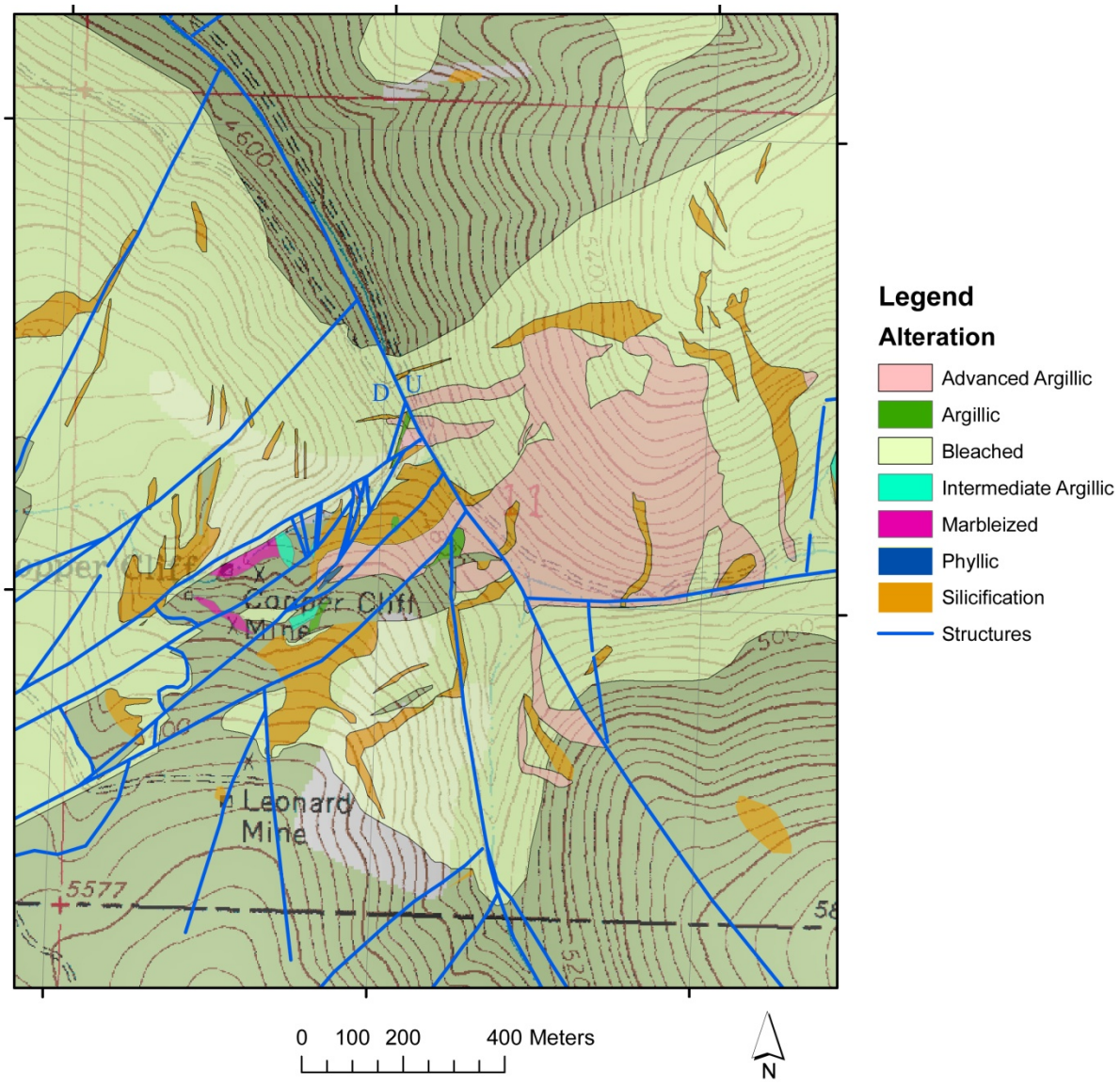


Figure 2.5. A detailed view of the complicated district center at Copper Cliff.

## 2.5. The Porphyry-to-Epithermal System Transition

The Anaconda report (Brannon et al. 1982) makes note of one of the more prominent alteration assemblages in the District, although it is referred to therein as “strong argillic”. The term advanced argillic has since come into wider use, and could also be typified by the outcrops in the center of the District, which exhibit an assemblage of silica and pink, high-Al alunite, with kaolinite, diaspore, and pyrophyllite (Ellsworth 1993). This type of alteration is common to high-level acid-sulfate epithermal systems, which as mentioned before forms much of the basis for continued interest in the Copper Cliff District (Simmons et al. 2005). The spatial association between acid-sulfate epithermal deposits and porphyry Cu-Au bodies has long been known, and is exemplified in papers such as Arribas et al’s 1995 study of the Lepanto Cu-Au deposits of the Philippines. Unfortunately, as noted by the authors of that work, a genetic relationship between the two has been much more difficult to determine.

Much of this difficulty results from that fact that porphyry ore deposits do not all exhibit identical characteristics. Features found in many deposits may not be found in all, and may not even be necessary for the development of the system type as a whole. Because of this, the associations between epithermal and porphyry styles of alteration and mineralization are best described in terms of analogs; systems that have undergone extensive study are good places to start in order to find general mineralization and alteration signatures that are common to the majority of porphyry systems. Past work has confirmed that porphyries, regardless of metallic content (e.g. Cu-Mo, Cu-Au, etc.), have a fairly uniform alteration zonation pattern, although commonly muddied by subsequent overprint and structural deformation. Many papers have also described the association of acid-sulfate epithermal base and precious metal deposits with underlying porphyry systems in many

localities worldwide (Sillitoe 1973, 1983; Wallace 1979; Rye 1993; Muntean and Einaudi 2001; Hedenquist et al. 1998). In general, these authors propose that acid-sulfate epithermal deposits are the surface expression of deeper hydrothermal processes associated with porphyry formation; an $H_2S$-rich vapor-phase rises from deep magmatic fluids to interact with meteoric water, and hence produce the sulfuric acid leaching of the overlying epithermal alteration.

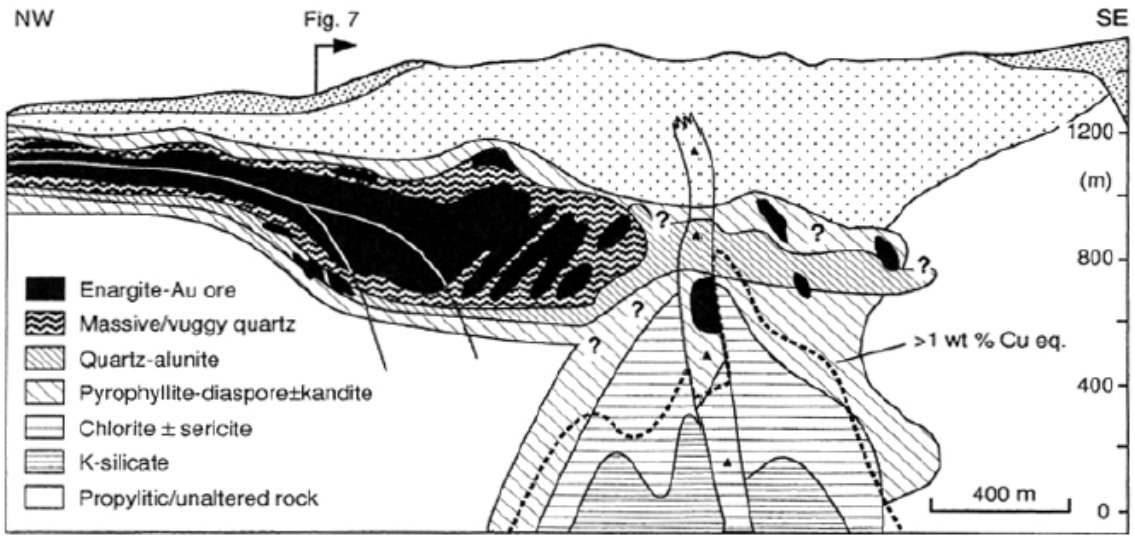


Figure 2.6. A schematic drawing of the Lepanto FSE deposit and its mineral and alteration associations. An example of a close spatial relationship between porphyry and epithermal styles of mineralization. Modified from Hedenquist et al. (1998)

Because of the high value of large, porphyry-type deposits, much work has been done to study their vertical and horizontal alteration zoning, often with the aim of developing a relationship between the porphyry and the epithermal (Sillitoe 1973; Lowell and Guilbert 1970; Rose 1970; James 1971), as well as to ascertain what goes into making a well-mineralized system. These studies, with the gathered knowledge of dozens of other authors, have put together models which describe the majority of the world's porphyry ore deposits. Exemplified best in Sillitoe's (1973) paper, such models generally describe zoning of K-

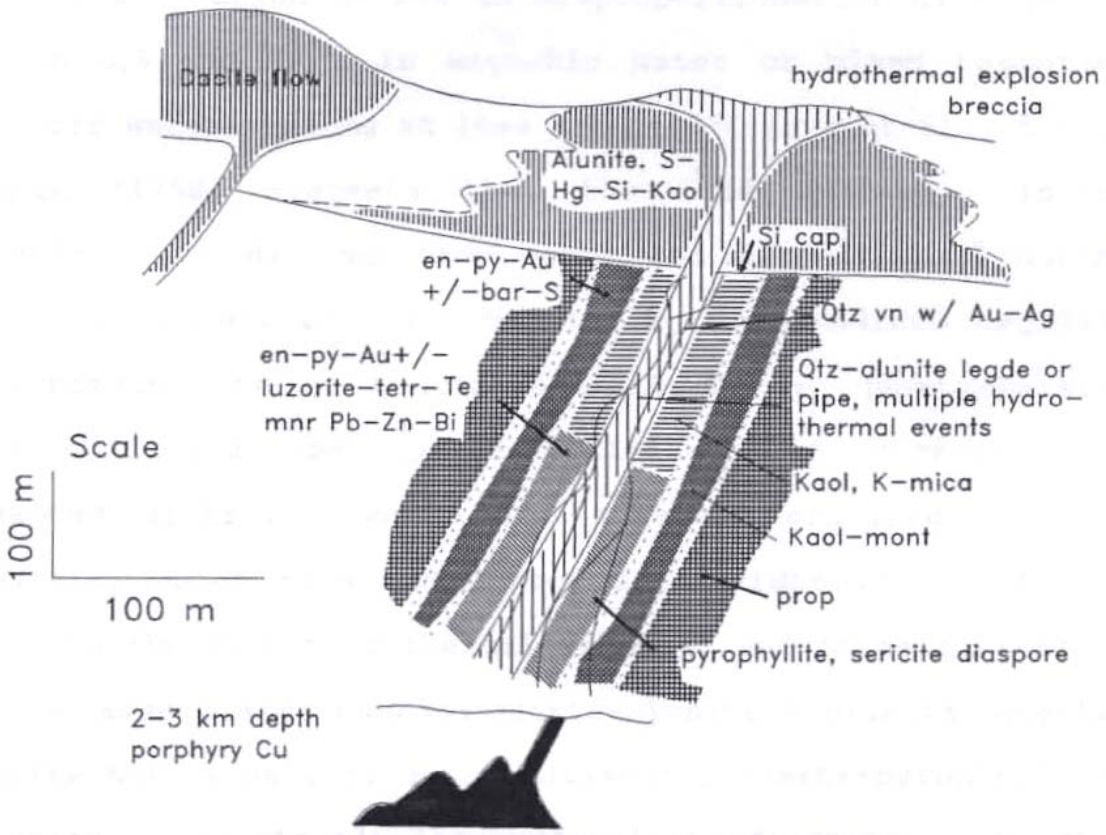


Figure 2.7. Schematic cross-section of an enargite-precious metal epithermal system, including mineralization and alteration. Modified from Bonham (1988).

silicate constructive, propylitic, sericitic, and advanced argillic alteration assemblages. These "alteration shells" are described as part of several famous Chilean deposits, while other papers cite the Kalamazoo District of Arizona (Lowell and Guilbert 1970), the Lepanto District of the Philippines (Hedenquist et al. 1998), and several deposits in western Nevada (Wallace 1979). The zoning of ore mineral assemblages largely follows these shells, and various authors have suggested a variety of exploration techniques to evaluate these models, though many are specialized to particular regions (Hedenquist et al. 1998; Muntean and Einuaudi 2001). Nonetheless, even given the differences that various porphyry deposits exhibit, it is at first reasonable to use these alteration and mineralization signatures to

determine the spatial position of a given sample within a system. Later, as more is learned about the deposit through drilling, petrography, and any number of other techniques, an often significantly-modified version of this model will be created. This study contributes to the development of such a specific model for the Copper Cliff system.

# 3. RESULTS

## 3.1. Alteration Mineral Distribution

Using the data collected in this study and by Kennecott Exploration geologists, two-dimensional plots of the surface distribution of alteration minerals were created. The PIMA™ SWIR spectrometer, coupled with The Spectral Geologist® spectral analysis software, returned a set of two minerals for most samples, ranked by relative abundance. A lesser number of samples contained only one mineral recognized by the spectrometer. This returned an extremely large number of combinations and it became impractical to plot the minerals themselves on maps, as no specific distribution was distinguishable. Efforts to classify each pair into a discrete alteration assemblage proved impossible, as two minerals is simply not enough to make a robust categorization. Therefore, The Spectral Geologist® was used to classify each spectrum by the amount of error as given by the software's internal scale for "certainty". Any spectra with errors greater than 200 were eliminated from the data set. This removed noisy and weakly-defined spectra, and reduced the error inherent in the data set as a whole, resulting in a much more probable group of alteration minerals with which to work.

After processing the data set, the list of the reported minerals numbered approximately 25. However, all but 7 of these appeared less than 10 times in over 1700

spectra, often as a secondary mineral in the reported pair, and were deemed to be either insignificant or a remnant part of the error in the original data set. Minerals important to delineating alteration zones in the district are halloysite, illite, alunite, kaolinite, montmorillonite, muscovite, and phengite, which represent a variety of temperature environments. Phengite is common in the distal parts of the district, and is likely not of hydrothermal origin; it is common in metamorphosed sediments such as those found in the country rock of Copper Cliff, and could not be interpreted to be part of the alteration halo of the District. Crystallinity differences between metamorphic and hydrothermal phengite were not able to be taken into account for lack of an acceptable standard from either source.

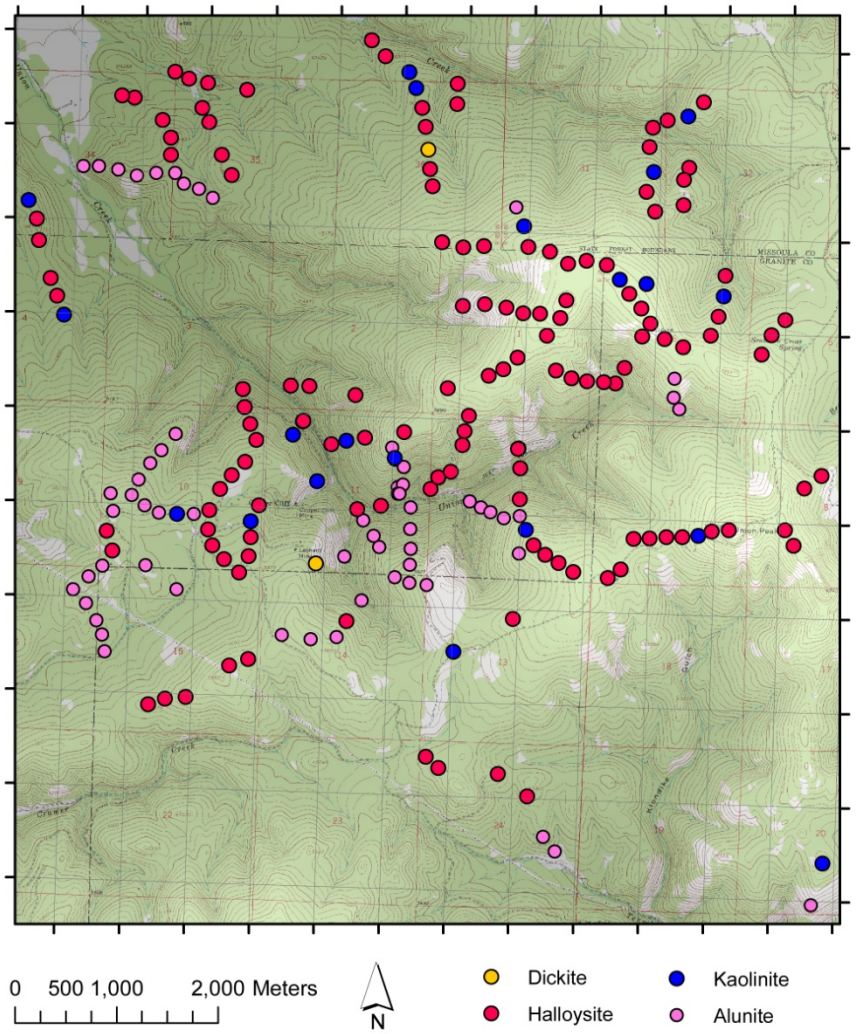


Figure 3.1. Major alteration mineral distribution at Copper Cliff, showing the occurrences of dickite, halloysite, kaolinite, and alunite as detected by the PIMA. Trends appear linear, as they follow ridges and valleys where transporting samples was easiest. This may have introduced a degree of bias, as ridgelines may exhibit different lithology than valleys.

The PIMA™ proved proficient at recognizing alunite at Copper Cliff. Because this mineral is characteristic of advanced argillic alteration, its distribution is mapped and compared with various metal distributions in an effort to define the District's thermal and mineralized center (Seedorf et al. 2005). In addition, an effort is made to correlate temperature to clay distribution, and the temperature-sensitive minerals halloysite (low), kaolinite (moderate), and dickite (high) are mapped (Figure 3.1). Compared to kaolinite and dickite, halloysite is far more common, indicating that there was little heat flux at this topographic level during the system's development. Alunite, in addition to appearing in the District's traditionally-recognized center, was detected by the PIMA in clusters up for 4 km away in almost every geographic direction. No historic prospects are found in these locations, and mapping was not carried out this far from the District center. The origin and extensiveness of these alunite occurrences is not covered by the study, though it is possible that they are simply extensions of a system that is far larger than previously thought.

## 3.2. Metal Distribution Maps and Models

Assay data for both surface and drill core samples were obtained from the exploration programs of Kennecott and Newmont. The Newmont program includes no surface sample assays, and core was only assayed for Au and Cu. In addition, Newmont drill holes only reached a minimum elevation of approximately 900 meters ASL. As a result, only three-dimensional models of Au and Cu included any Newmont data; Kennecott's assays were used exclusively in the creation of surface distribution maps and other 3D models.

Kennecott's surface data (Figure 3.2) represents a useful distribution of points that can be used to draw conclusions about the concentrations of metals in various parts of the

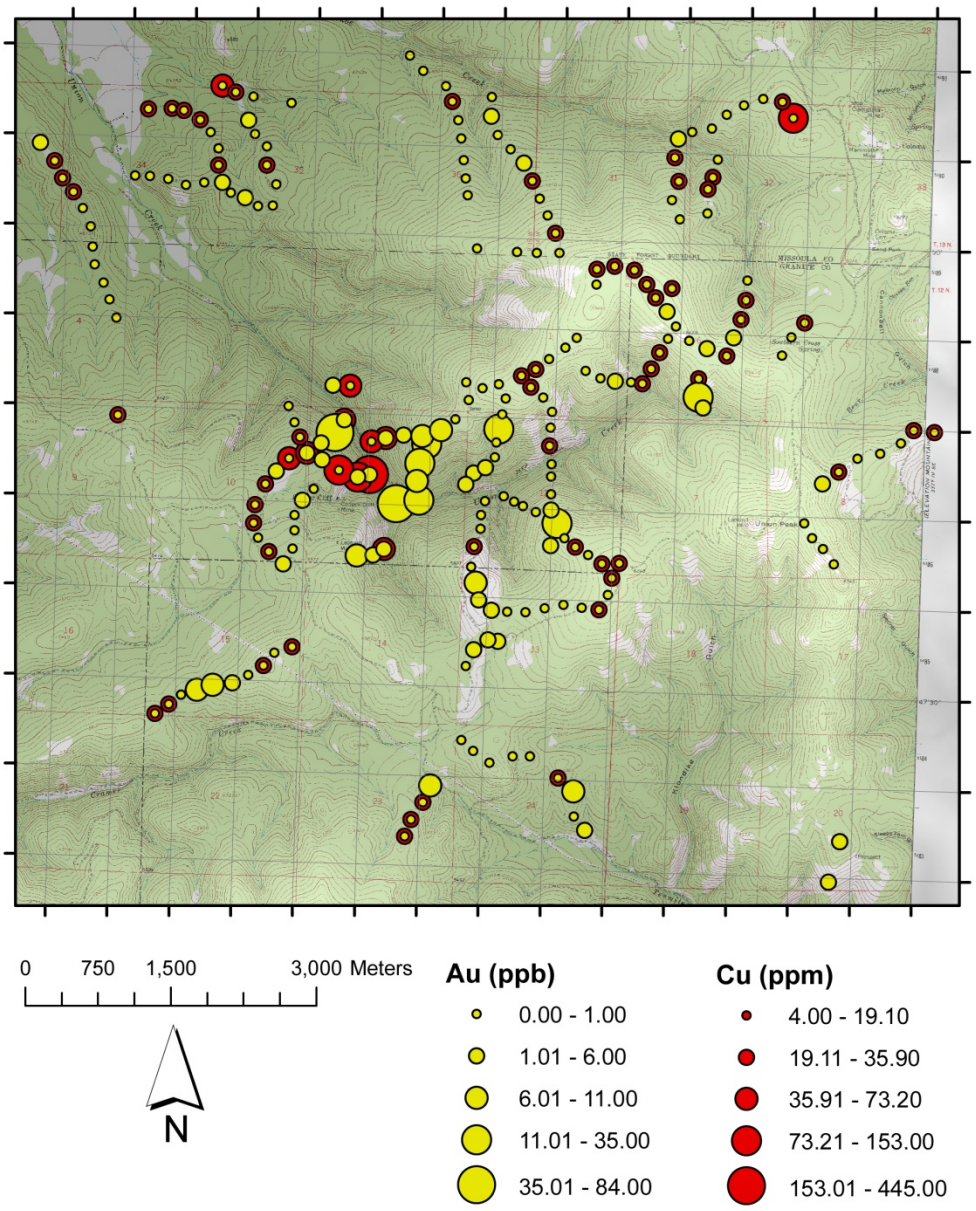


Figure 3.2. Map of surface distribution of gold and copper at Copper Cliff. Copper is detected at all locations, though often gold is limited to barely over the detection level. With gold plotted on top of copper, it is shown that comparatively large amounts of gold are located in the center of the District. Darker symbols that appear like bullseyes are trace Au plotted on top of Cu.

District. Metals investigated for zoning relationships were limited to those known to be important indicators in other porphyry-style systems, and consisted of copper, gold, lead, and zinc (Figures 3.3-3.5). Other metals, such as Mo, Mn, and Ag, as well as volatiles like As

and Sb, were available for study. However, all of these elements but Mo is known to mimic the distributions of Cu, Au, Pb, or Zn in porphyries, and little can be gained from their addition to this work. Concentrations of molybdenum at Copper Cliff are very low; concentrations above 100 ppm are rare, and the highest recorded is 261 ppm. This, coupled with numerous spikes and troughs in concentration, makes Mo an ineffective illustrator of metal zoning at Copper Cliff. A correlative distribution of copper and gold was also examined, with the ratio of Cu:Au plotted in three dimensions (Figure 3.6).

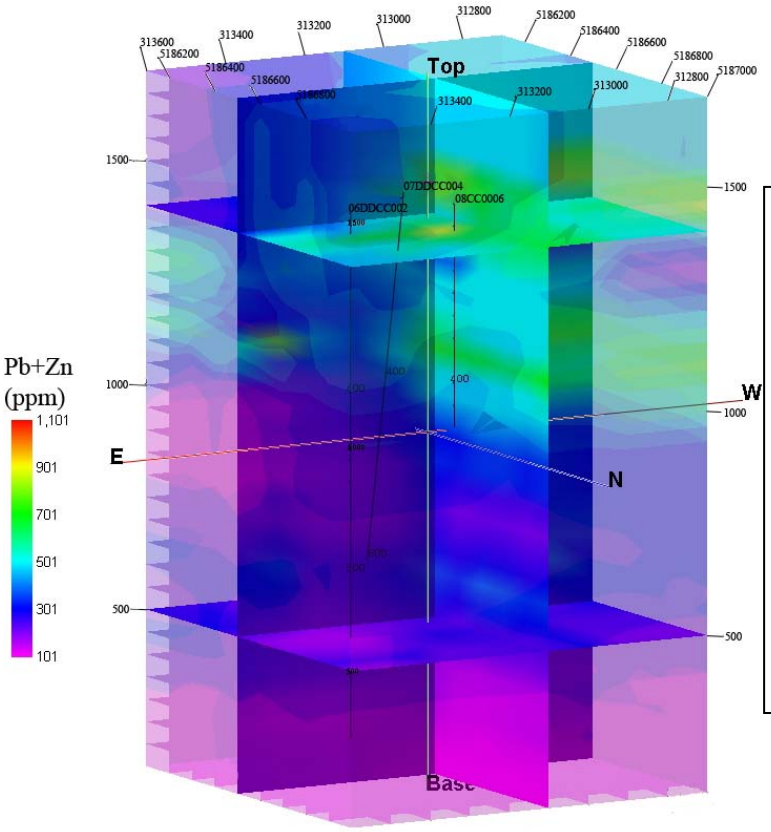


Figure 3.3. Model of the distribution of Zn and Pb in the Copper Cliff subsurface. These elements are typically found on the margins of porphyry deposits. Although current drilling has focused on the center of the system, this pattern is already apparent; the deep parts are low in Zn+Pb, and the upper and outer parts are enriched.

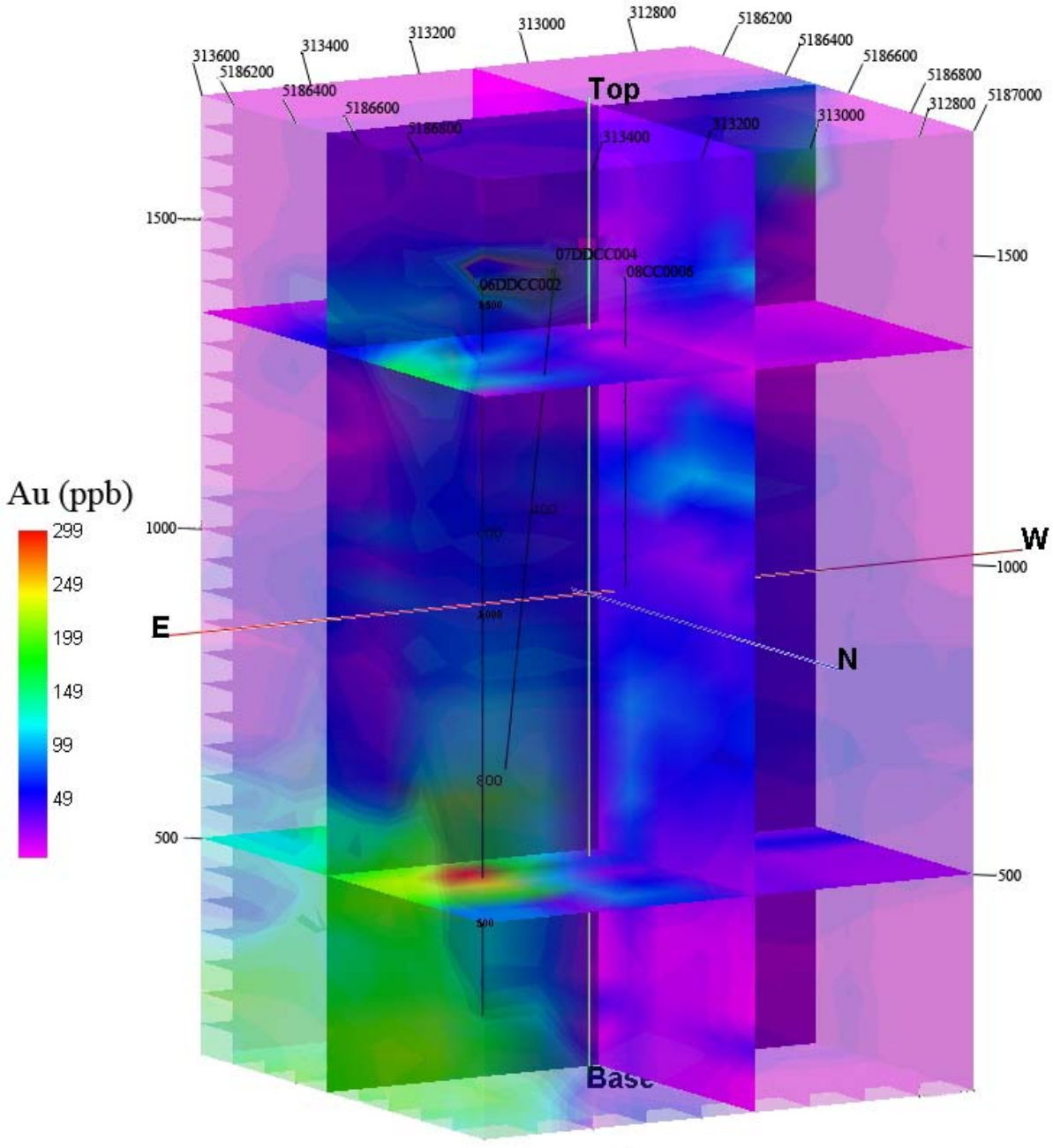


Figure 3.4. Distribution of subsurface gold at Copper Cliff follows the expected distribution of an intact porphyry-to-epithermal transition. Elevated values are apparent at high levels in the system, while lower down they again increase after a gold-poor midsection of some 700 meters.

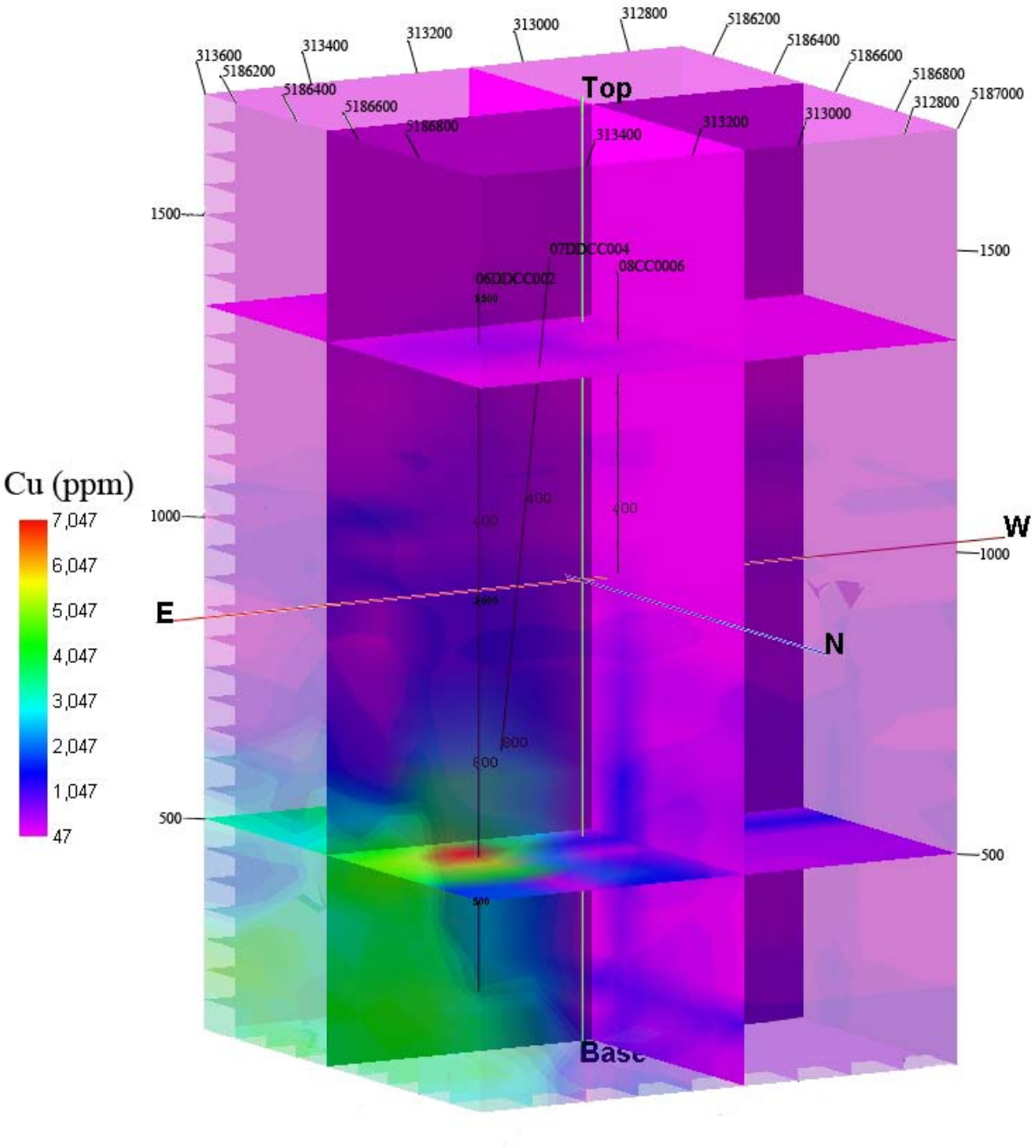


Figure 3.5. Copper in the District, while historically mined at shallow levels, is concentrated in the deepest parts of the system, below approximately 500 meters ASL. Potential exists for more mineralization at greater depths.

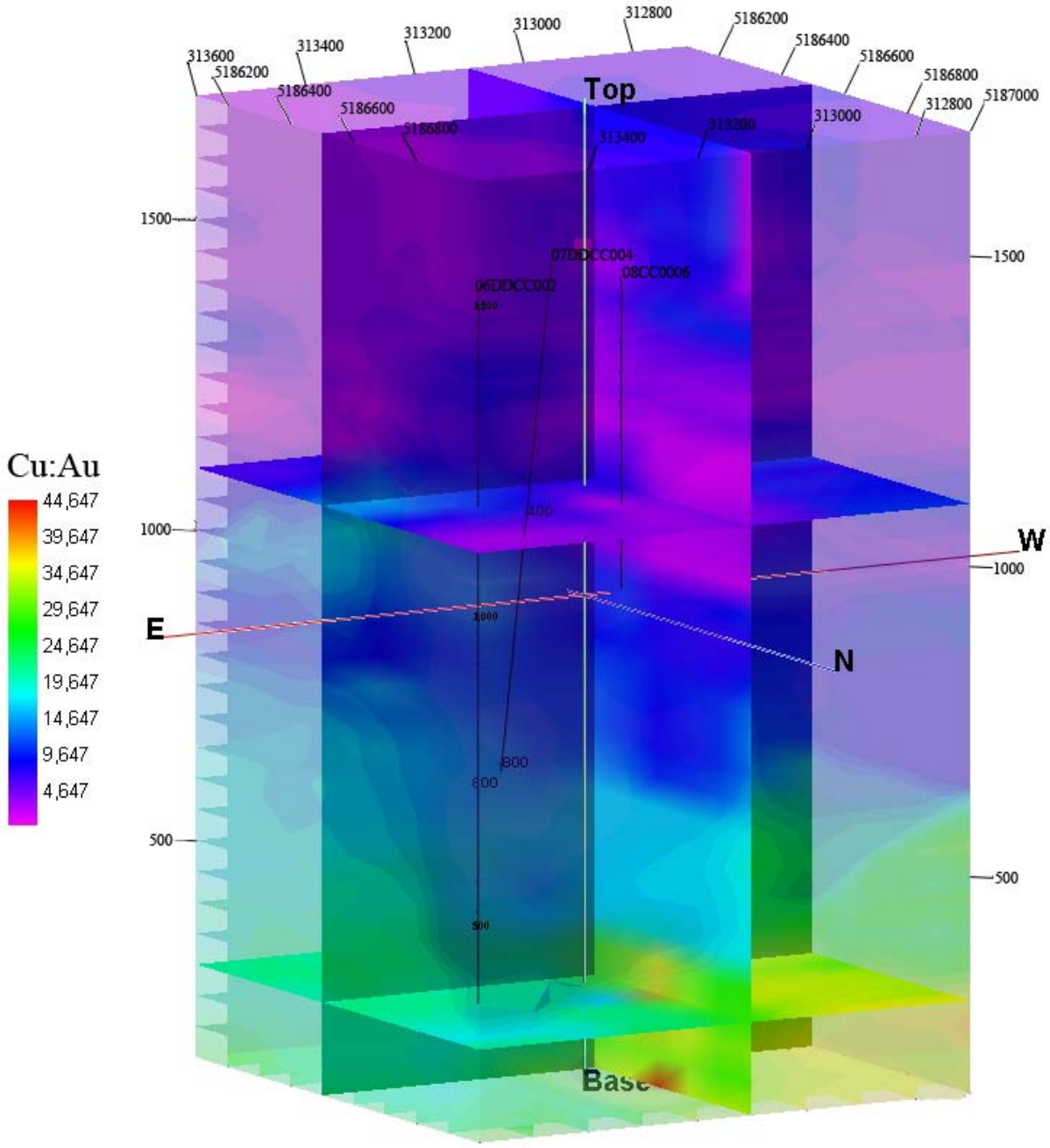


Figure 3.6. The Cu:Au ratio at Copper Cliff increases dramatically in the lower part of the known system, due to the marked increase in Cu concentrations and the slower rise in Au. Gold at Copper Cliff is concentrated in this deep part of the system below 500 meters ASL.

## 3.3. Petrography

Petrographic sampling was undertaken with a two-fold objective: correlate visible textures and mineralogical overprinting relationships with PIMA™ spectra, and characterize the deposit in terms of said relationships and mineralogy. Samples representative of drill core from holes 002, 003, 004 and 005 were taken. Before these samples were made into polished thin sections, up to three SWIR spectra were obtained from each using the PIMA™. In all, 55 sections were analyzed: 14 in hole 002, 9 in hole 003, 18 in hole 004, and 14 in hole 005 (Figure 3.7)

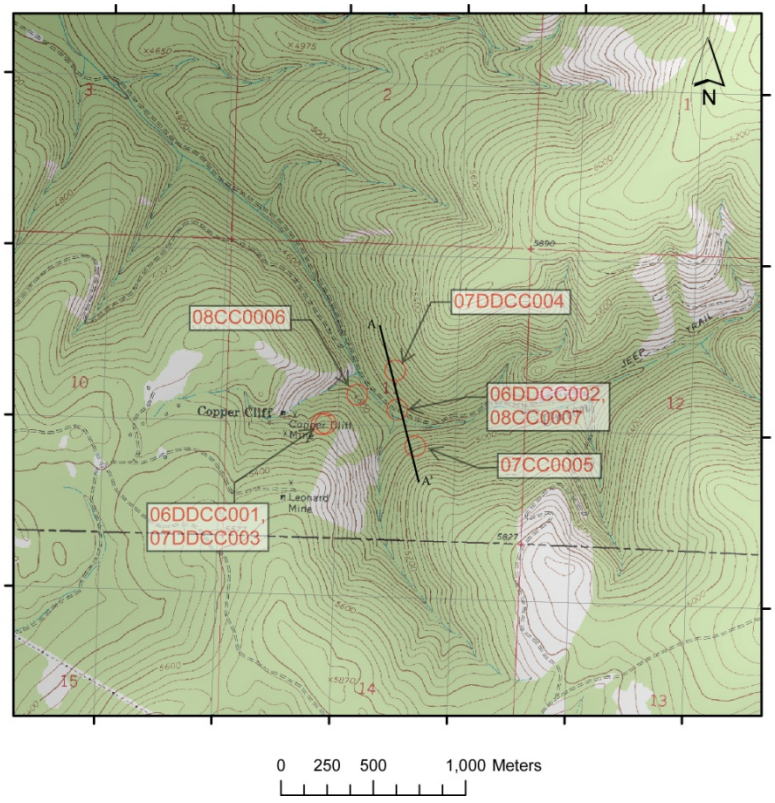


Figure 3.7. Map of Kennecott drill holes completed from 2006 to 2008. Hole 06DDCC001 was aborted at 50 meters depth, and 003 was begun from the same pad. Hole 08CC0006 was lost while crossing the thick Union Creek Fault zone at an oblique angle, and hole 0007 was drilled from pad 002 at an angle to intersect the lost ground. Except for this and hole 004, which was drilled at 77.5° dip to the NE, all holes are vertical. Section A-A' refers to Figure 5.1.

### *Hole 06DDCC002*

Originally drilled in 2006, this hole was re-entered and extended down to approximately 250 meters ASL. Sampling was begun at 736 meters in quartz latite porphyry with strong phyllic alteration, characterized at Copper Cliff by replacement of magmatic

aluminum silicate minerals by poorly-ordered white phyllosilicates (illite, muscovite, and sericite), silicification of the matrix, and pyritization, both as disseminations and in quartz veins (Figure 3.9, part A). In such cases, mafics have been extremely eroded, appearing rounded and pitted. Overprinting becomes apparent by 690 meters, with phyllic superimposed on K-silicate biotite-constructive alteration (KSBC) (Figure 3.9, part D). Often termed "potassic" alteration, shreddy biotite is the only potassium silicate mineral added to the assemblage at Copper Cliff. At 690 meters, both hydrothermal and magmatic biotite is being altered to white phyllosilicates, with pyrite closely associated at former mafic sites (Figure 3.9, part C).

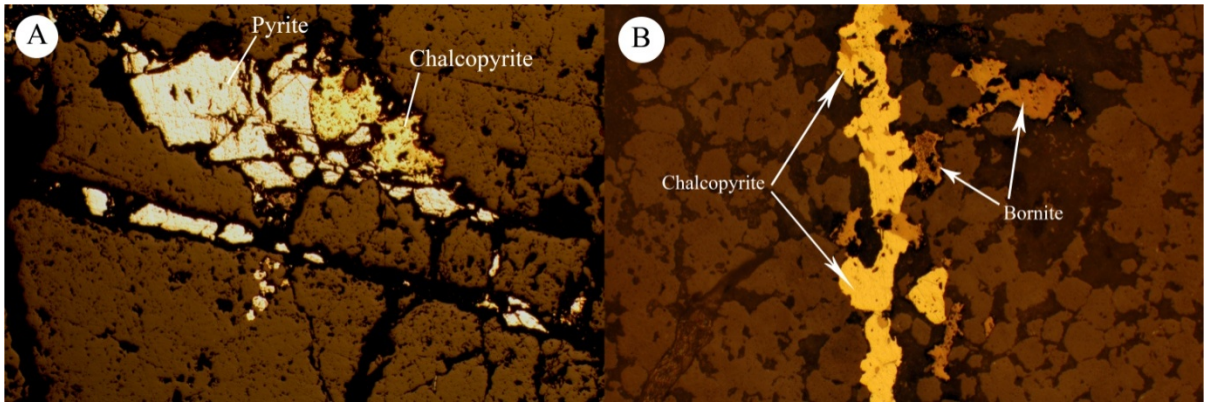


Figure 3.8. Sulfides common below 550 meters ASL, seen in reflected light. A) Section of veinlet at 572.5 m ASL, comprising pyrite and chalcopyrite in a 70:30 ratio. Cpy appears as intergrowths and discrete grains in vein. FOV is 1800 µm. B) Sample from section averaging 0.75%-wt Cu at 407.37 m ASL, with bornite and chalcopyrite comprising the bulk of veinlets, along with pyrite (not pictured). Photo width is 800 µm.

From 645 meters down to approximately 415 meters, strong phyllic alteration includes a significant component of smectite and low-temperature clays, with traces of minerals associated with advanced argillic alteration, such as alunite, kaolinite, and pyrophyllite. These minerals are absent from 415 meters to the hole's termination at approximately 275 meters, in which KSBC alteration becoming stronger with depth and is

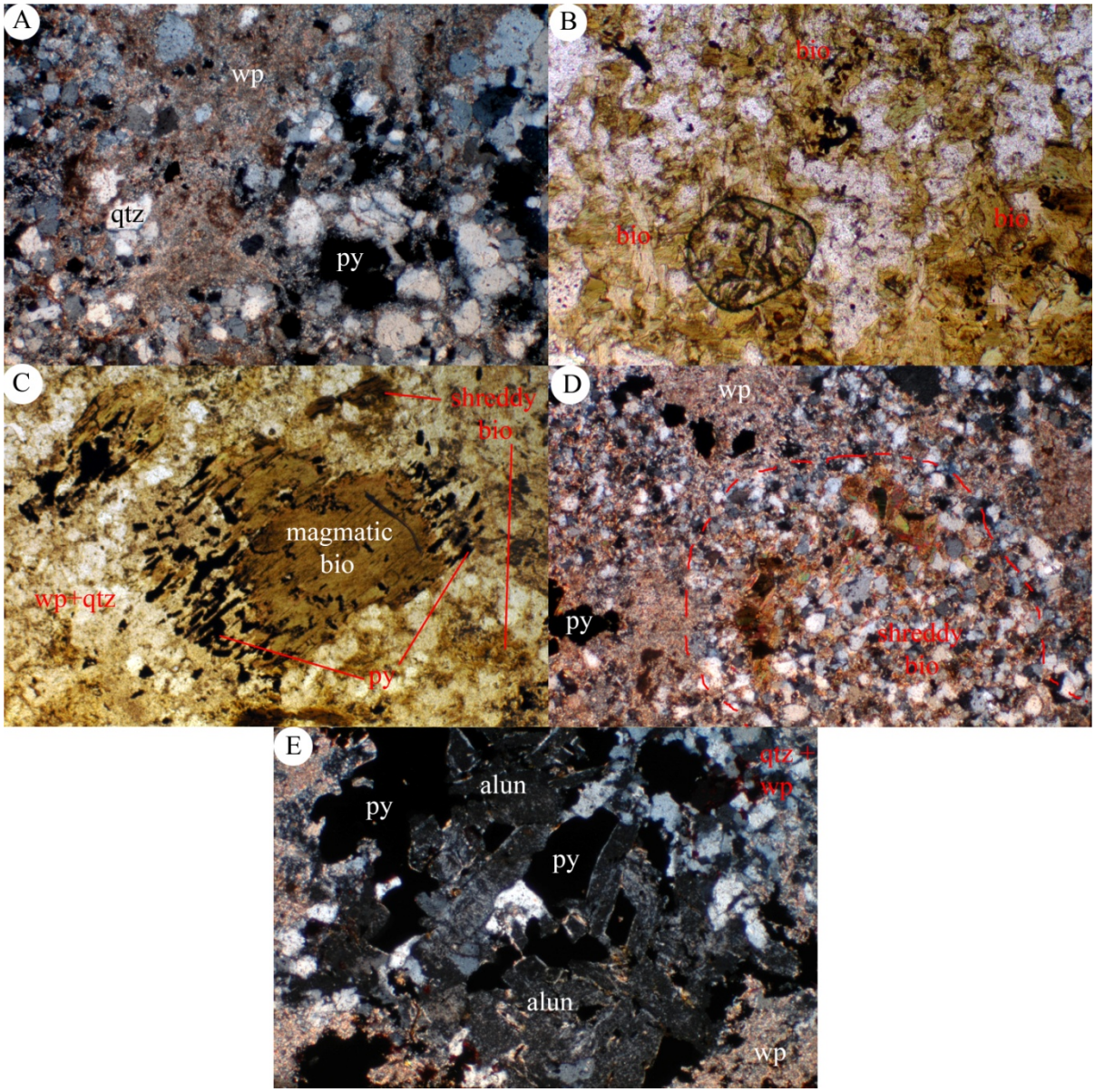


Figure 3.9. Alteration assemblages common in the lower sections of hole 06DDCC002. Photo widths in all are 1800 µm. A) Strong phyllic alteration under polarized light at 472.24 meters ASL, with white phyllosilicate (wp), quartz (qtz), and pyrite (py) comprising over 95% of the sample. B) Strong KSBC alteration under plane light at 278.49 meters, with a weak phyllic overprint. The hole ended in this assemblage. C, D) Examples of KSBC alteration overprinted with phyllic, at 691.1 m (plane light) and 387.36 m (polarized light), respectively. This helps illustrate the wide distribution of this overprinting relationship. E) Anomalous replacement of alunite crystal lathes (alun) by smectite under polarized light at 353.57 meters, associated with phyllic alteration.

overprinted with phyllic to varying degrees (Figure 3.9, part B). A singular but significant deviation occurs at 350 meters, in which well-developed alunite crystals have been completely replaced with low-temperature clays (Figure 3.9, part E). Specular hematite is commonly found associated with Cu-bearing sulfides below approximately 550 meters ASL, which include chalcopyrite, bornite, and small amounts of chalcocite (Figure 3.8).

*Hole 07DDCC003*

Collared SE of hole 002, this hole encountered weak propylitic alteration, with magnetic and smectite, down to 1450 meters. In this area, specular hematite is seen replacing magnetite (Figure 3.10). Below this weakly-altered zone and down to 1000 meters ASL, advanced argillic alteration is the primary style, with overprinting by phyllic increasing with depth all the way to the bottom of the hole at 900 meters (Figure 3.11). Pyrite increases with depth in this section, from trace to ~1%-vol. The hole is primarily in latite porphyry intrusive, and amphiboles replaced by white phyllosilicates are common. These are seen again in hole 07CC0005, although they are not observed in any hole north of the Union

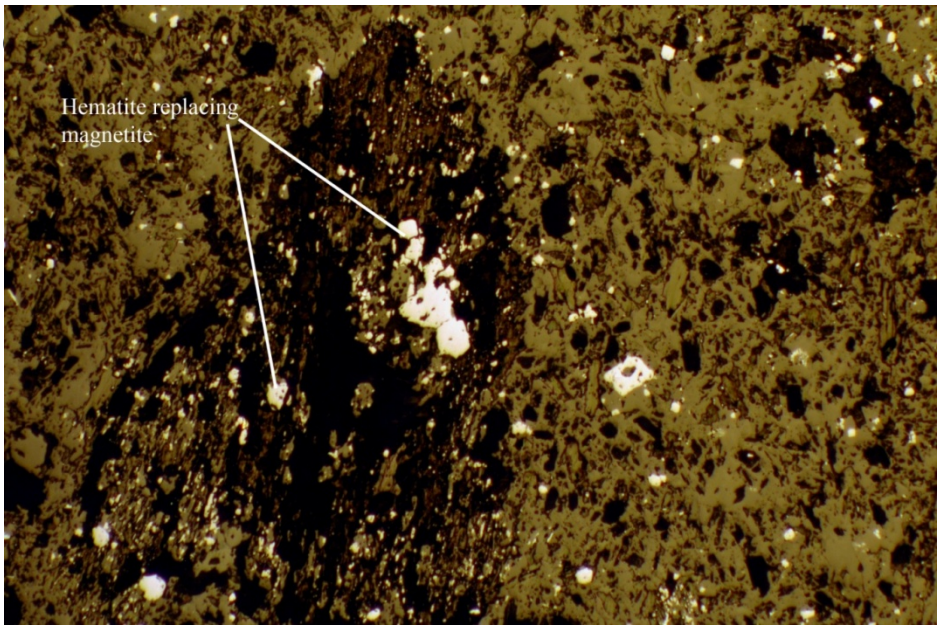


Figure 3.10. Reflected light photo of specular hematite replacing magnetite at 1488.68 meters. The replacement is deduced by the crystal shape of the former magnetite, and the optical properties of the specular hematite. Photo width is 1800 µm.

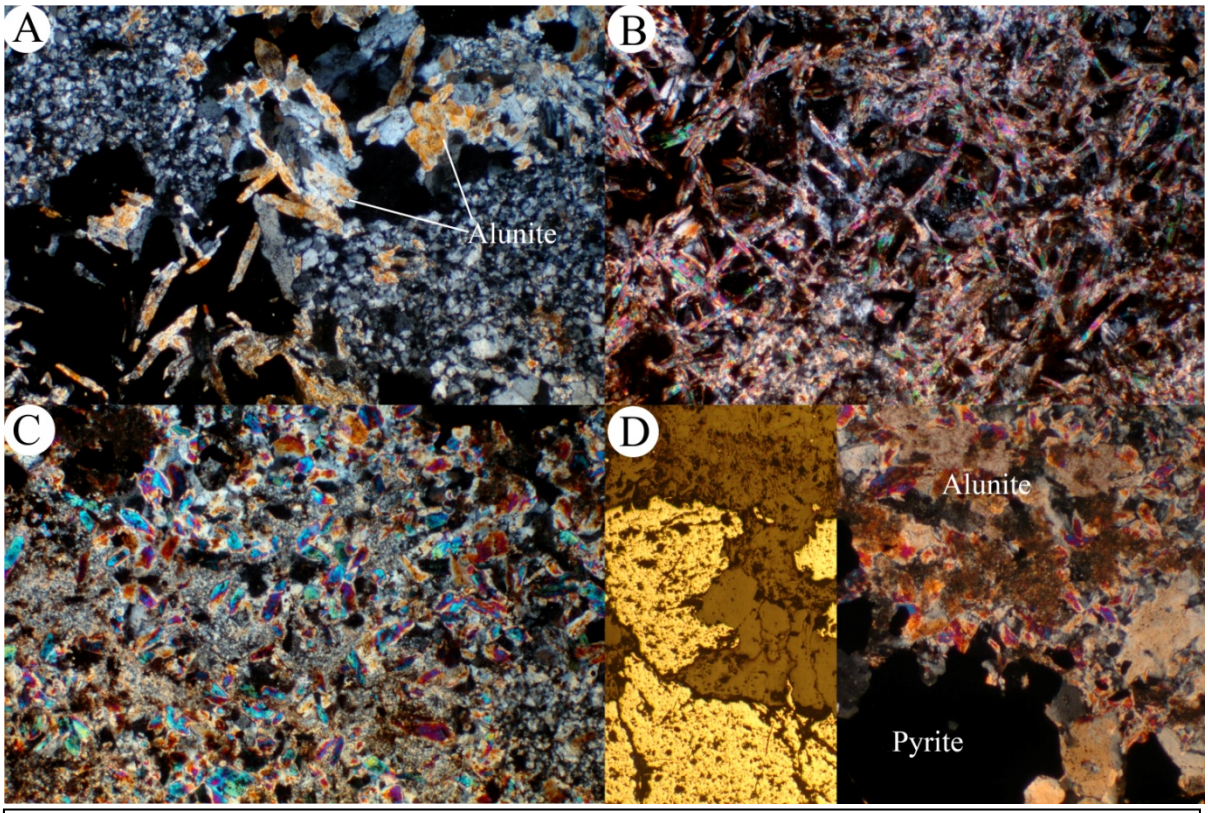


Figure 3.11. Photos of advanced argillic alteration (alunite) at various elevations in hole 07DDCC003. Photo widths in all are 1800 µm, under polarized light. Part D includes a snip of a photo taken under reflected light. A) 1299.90 meters, alunite with white phyllosilicate and quartz. B) 1235.40 meters, long alunite crystals replacing feldspar sites in latite porphyry. C) 1081.81 meters, large patch of alunite crystals covering large swaths of sample. D) Alunite and kaolinite closely associated with pyrite at 1027.80

*Hole 07DDCC004*

This hole, more densely sampled than others, shows the rapid alteration style changes characteristic of the Copper Cliff system. It begins at 1525 meters in advanced argillic alteration, with alunite, kaolinite, chalcedony, and pyrophyllite (Figure 3.12). Down to 1075 meters, advanced argillic remains the dominant alteration type, with short 10 to 20-meter intercepts of intermediate argillic, characterized by chlorite and low-temperature clays with

shreddy biotite. Below 1075 meters, advanced argillic begins to be interspersed with phyllic-

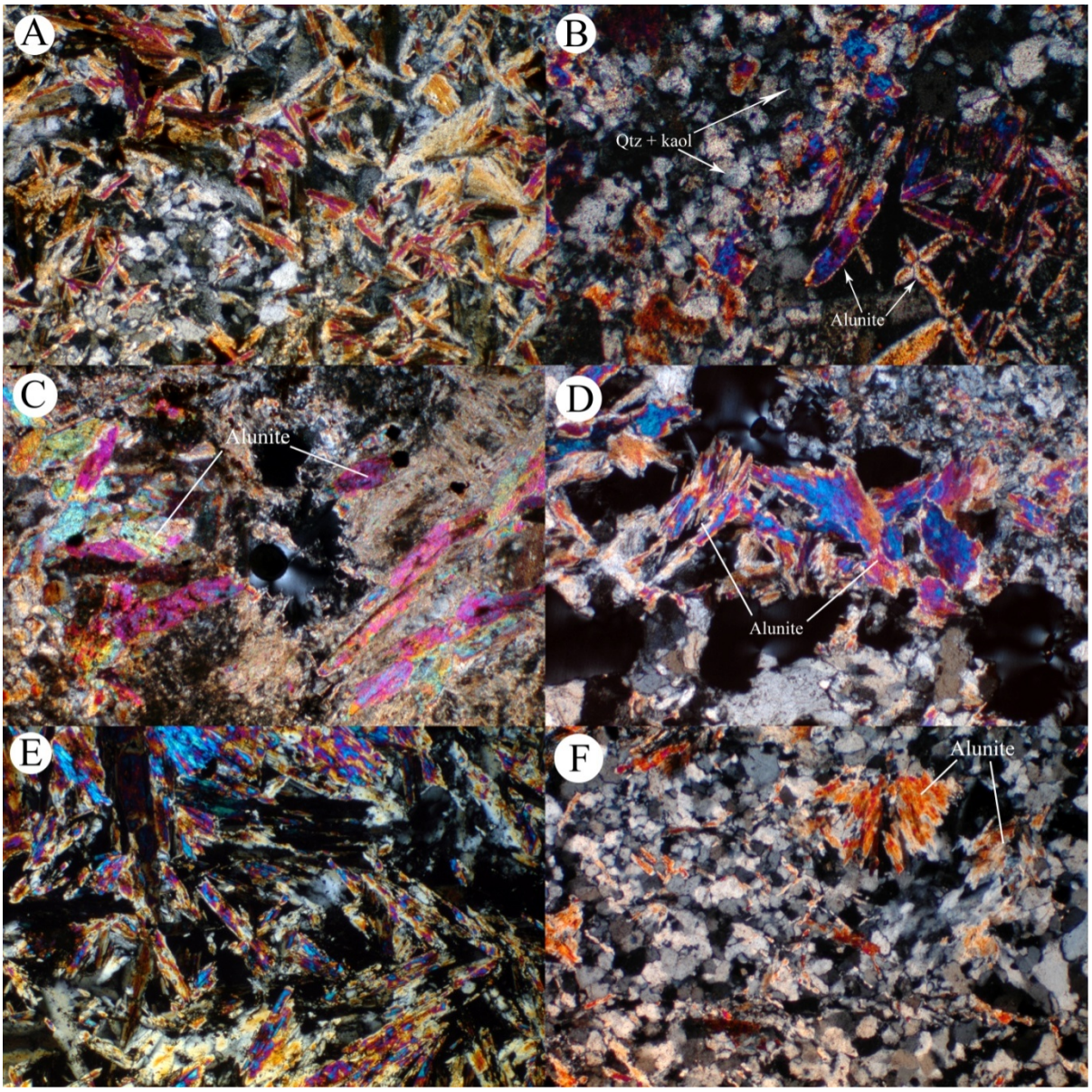


Figure 3.12. Examples of advanced argillic alteration from hole 07DDCC004, in which strong advanced argillic persisted with little overprint from 1525 meters down to approximately 1075 meters, and is present in significant amounts even lower. In photos where alunite is not labeled, the mineral comprises over 90% of the photo (1800 µm wide). Samples are from A) 1479.99 meters, B) 1367.30 meters, C) 1165.01 meters, D) 1022.20 meters, E) 1005.81 meters, and F) 909.00 meters.

overprinted KSBC alteration. This phyllic overprint was found to be structurally controlled, and developed "bleached" halos (normally on the order of 1-2 centimeters wide) around quartz-sulfide veinlets, in which magmatic and hydrothermal biotite had been altered to white phyllosilicates.

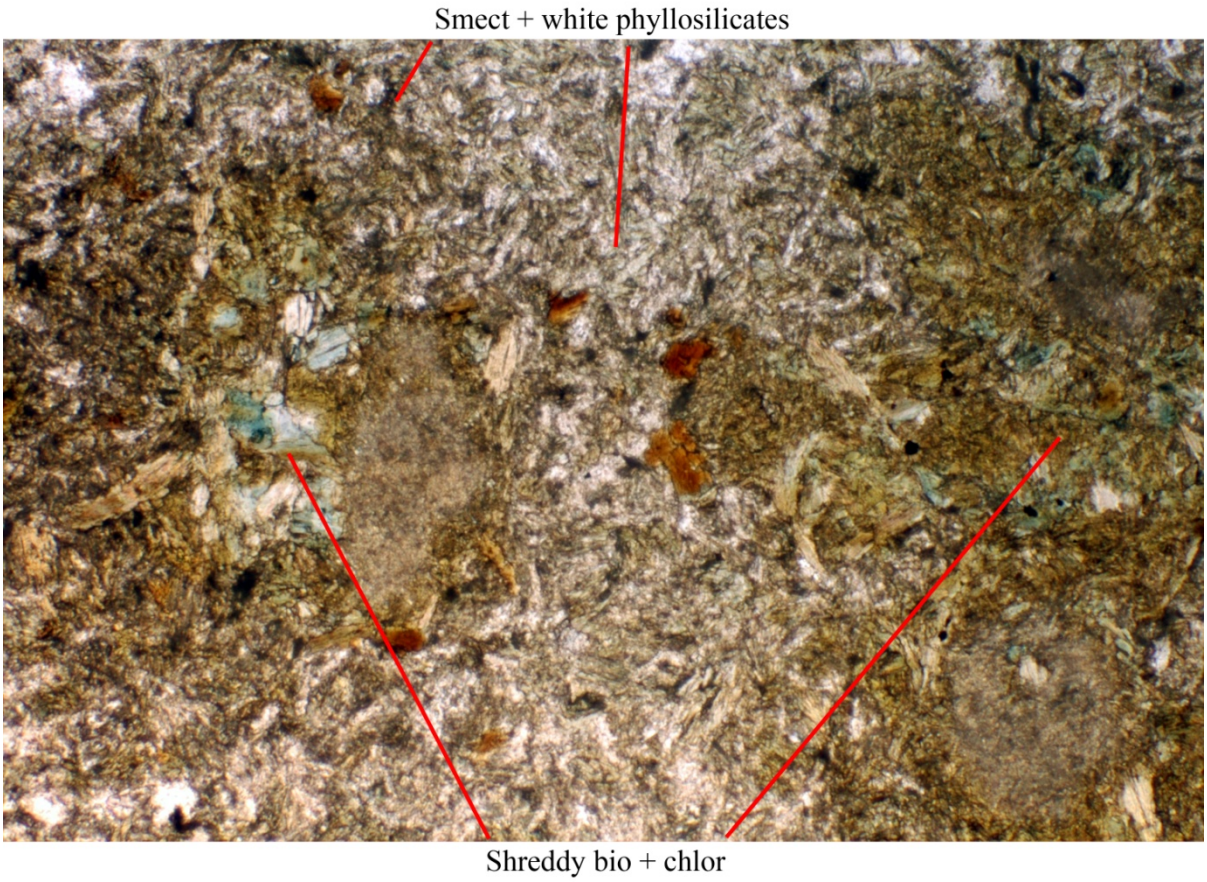


Figure 3.13. Example of strong intermediate argillic alteration from 727.43 meters ASL in hole 07DDCC004. This sample exhibits significant addition of chlorite, smectite, and shreddy hydrothermal biotite. Remnant magmatic biotite can be seen as chocolate-brown grains at the photo's center. Photo width is 1800 µm.

Advanced argillic ceases to be the dominant alteration type below 1075 meters, although it persists in nearly every sample to the bottom of the hole at approximately 800 meters. This is most prominently demonstrated at 1005 meters, where the hole intersects a

vein of solid coral-pink alunite 10 centimeters wide (Figure 3.12, part E). Alteration types encountered in the lower 200 meters of the hole include intermediate argillic, phyllic, and KSBC or advanced argillic alteration, both overprinted with phyllic. The hole ends in intermediate argillic (Figure 3.13).

*Hole 07CC0005*

In the top 150 meters, this hole exhibits alteration types not seen elsewhere in the district. Above 1450 meters is a combination of intermediate argillic-altered latite porphyry and bleached, sericitized Garnet Range sediments. In the next 85 meters, limestone skarn with heavy garnet and pyroxene is encountered, along with hornfels of the same protolith. Beyond approximately 1325 meters to the bottom of the hole at 640 meters, phyllic-altered latite porphyry becomes the dominant assemblage. However, unlike other phyllic alteration found in other holes, phyllic in hole 0005 is always accompanied by varying concentrations of smectite, carbonate, and specular hematite. Specular hematite is found in nearly every sample, and appears to have been overprinted with phyllic alteration, as evidenced by bleached quartz vein halos in which pyrite is dominant and specular hematite is absent (Figure 3.14).

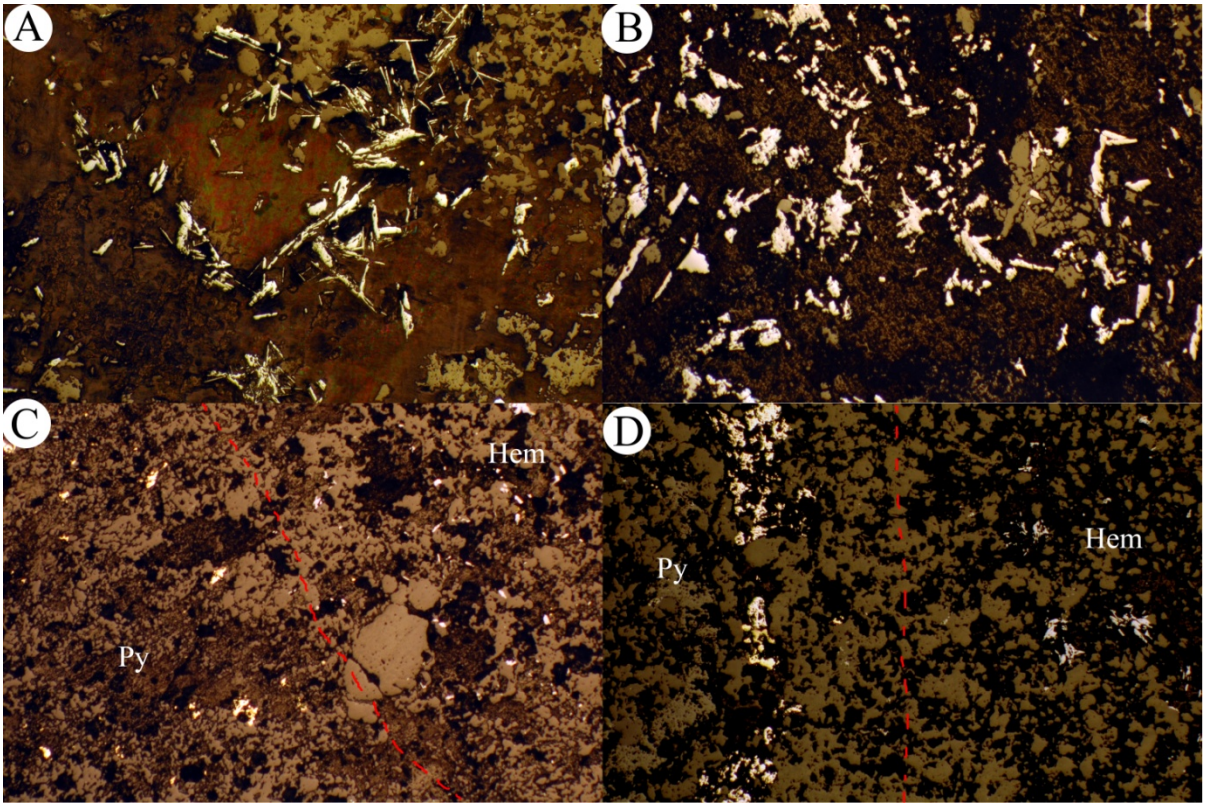


Figure 3.14. Examples of specular hematite occurrences common in hole 07CC0005. Parts A and B (948.10 meters and 1162.04 meters, respectively) show frequently-seen textures, including tabular (A), and blocky (B) specular hematite grains. Parts C and D (999.59 and 956.07 meters) show pyrite's overprint relationship with specular hematite that is common in the lower parts of the hole. Dotted red lines delineate the rough border between pyrite-only and specular hematite-only sections of the sample. As shown best in part D, this overprint is associated with quartz-pyrite veinlets. Width of view is 1800 µm in all photos.

## 3.4. Stable Isotope Geochemistry

A total of 12 samples of alunite were analyzed by mass spectrometry to determine their sulfur isotopic ratios; 6 from the surface or near-surface, and 6 from lower elevations (Table 3.1). Several additional samples that are not shown were analyzed; however, these were discarded due to a large amount of pyrite contamination of the alunite sample. As pyrite is often closely associated with alunite (Figure 3.11, part D), it was frequently

impossible to completely separate the two. Samples of alunite and pyrite were purified by sieving, followed by hand-picking under a binocular microscope.

| Sample | Formula | Mineral | Identifier | Elevation (m) | Corrected $\delta^{34}S$ | Notes |
|---|---|---|---|---|---|---|
| C4 | $KAl_3[(OH)_3\|SO_4]_2$ | Alunite | 07DDCC004 | 1005.81 | 21.1 | Pure alunite |
| B11 | $KAl_3[(OH)_3\|SO_4]_2$ | Alunite | 07DDCC003 | 1081.81 | 16.3 | Pyrite contaminated (moderate) |
| B1 | $KAl_3[(OH)_3\|SO_4]_2$ | Alunite | 07DDCC004 | 1166.11 | 15.4 | Pyrite contaminated (moderate) |
| A9 | $KAl_3[(OH)_3\|SO_4]_2$ | Alunite | 07DDCC004 | 1205.88 | 18.0 | Pyrite contaminated (light) |
| B9 | $KAl_3[(OH)_3\|SO_4]_2$ | Alunite | 07DDCC003 | 1244.4 | 19.2 | |
| B4 | $KAl_3[(OH)_3\|SO_4]_2$ | Alunite | 07DDCC004 | 1479.99 | 20.8 | Pure alunite |
| B10 | $KAl_3[(OH)_3\|SO_4]_2$ | Alunite | 40100789 | 1491.01 | 21.0 | |
| A12 | $KAl_3[(OH)_3\|SO_4]_2$ | Alunite | 40100822 | 1510.69 | 18.4 | Pyrite contaminated (light) |
| B6 | $KAl_3[(OH)_3\|SO_4]_2$ | Alunite | 40100793 | 1520.11 | 22.1 | |
| B5 | $KAl_3[(OH)_3\|SO_4]_2$ | Alunite | 40100786 | 1619.79 | 19.9 | |
| B2 | $KAl_3[(OH)_3\|SO_4]_2$ | Alunite | 40100813 | 1681.62 | 19.8 | |
| B7 | $KAl_3[(OH)_3\|SO_4]_2$ | Alunite | 40100812 | 1724.23 | 19.0 | |
| C1 | $FeS_2$ | Pyrite | 07DDCC004 | 949.87 | -11.0 | |
| B12 | $FeS_2$ | Pyrite | 07DDCC004 | 1166.11 | -12.6 | |

Table 3.1. Information on the samples of alunite and pyrite analyzed for stable isotopes. 8 standards with known isotopic ratios of various sulfide and sulfate species were run prior to the samples, in order to correct the raw $\delta^{34}S$ value for error during the analysis.

The two purest samples of alunite, B4 and C4, have an almost identical $\delta^{34}S$ value, despite being separated by almost 475 meters of elevation. Samples in Table 3.1 that are labeled as “pyrite contaminated” contained fine-grained pyrite that was difficult to separate from the alunite. Their approximate percent pyrite content was noted visually, and was found to correlate with the lighter isotopic values obtained for these samples. Alunite samples have values between 19 and 22‰, while pyrite is far lighter at -11 and -12.6‰ (Figure 3.15).

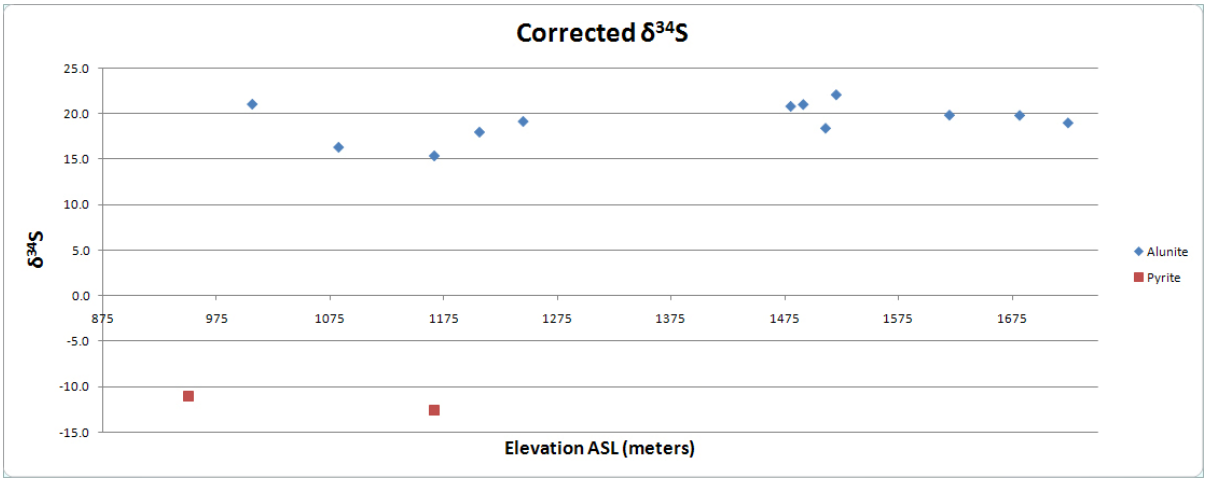


Figure 3.15. Plot of alunite and pyrite isotopic values with elevation. Pyrite, or sulfide, is exceptionally light, while sulfate (alunite) remains high through the entire column of the sampled part of the Copper Cliff system. No trend with elevation is noted

# 4. DISCUSSION

## 4.1. The PIMA

Originally, it was expected that alteration assemblages could be effectively and rapidly mapped using the PIMA™. However, processing of the data revealed certain limitations to this approach, as it was found that the presence of sulfides would produce such noisy or flat spectra that the results were rendered useless. Because of the abundance of pyrite in many sections of drill core, it was often impossible to avoid this noise. The link between sulfide content and noise level in the spectra was empirically determined during the project, although it is likely that a mineral closely associated with pyrite is to blame; sulfides, being non-hydrous, should be invisible to the PIMA™. Regardless, when these noisy spectra were processed with the software used onsite for mineral identification, the result would be either aspectral, or an unlikely pair of minerals which upon manual inspection were either an improbable combination or a poor match to the reference spectra. As a result, over ⅓ of the collected spectra were discarded. This seems to be at odds with other researchers' experience with the PIMA™, as such difficulties were not referenced in works such as Yang et al. (2005) and Mars and Rowan (2006). Additional experimentation is necessary in order

to deduce the source of error in these spectra.

However, the instrument proved useful at Copper Cliff for a certain set of tasks. Where clays and other alteration minerals occurred in high concentration or with relatively little pyrite, they could be readily identified and mapped. This was particularly common in the case of alunite and kaolinite in advanced argillic alteration, and illite and muscovite in phyllic alteration. Unfortunately, due to the SWIR spectroscopy's reliance on the O-H bond within minerals for analysis, non-hydrous or weakly-hydrous alteration assemblages characterized by minerals such as biotite, orthoclase, quartz/chalcedony, sulfides, and iron oxides are invisible to the instrument, and instead tend to introduce noise into the spectra, masking other identifiable minerals. These assemblages were instead identified through petrography.

## 4.2. Alteration

Ellsworth (1993) and Newmont Exploration established the existence of a "bullseye" of advanced argillic alteration at Copper Cliff, with a large halo of propylitic alteration. However, data collected during this project supports a much more widespread occurrence of alunite, and a non-propylitic area around the District center. In Figure 3.1, this center is shown as a close collection of alunite-bearing samples, and represents the main advanced argillic-altered area characterized by alunite, kaolinite, and chalcedony, with minor amounts of pyrophyllite and diaspore. However, as mentioned previously, clusters of alunite are not constrained to this bullseye, but instead are found in several places throughout the District at large. In addition, PIMA™ data presented here as well as recent mapping by Kennecott geologists (Figure 2.4) has shown that the dominant alteration type surrounding the central

alunite occurrence is not propylitic alteration, but sericitization, termed “bleaching” at Copper Cliff because of the white color this assemblage lends to affected Garnet Range sediments. Nearly all intrusive rocks exposed at the surface exhibit either advanced argillic alteration or heavy silicification, assemblages that are characteristic of the upper portions of some porphyry systems (Sillitoe 1973). Intermediate argillic-altered latite porphyry outcrops to the east of the central alunite zone, and represents the only surface exposure of an alteration type that normally comprises an outer shell of an ideal porphyry deposit. High and low temperature minerals (dickite and halloysite, resp.) show no zoning relationships on the surface, although it should be noted that dickite is conspicuously absent from the center, and presumably the hottest, section of the District. This is especially significant when combined with stable isotopic data and petrography.

Since the PIMA™ proved ineffective at mapping all alteration types that are present in the subsurface, petrographic interpretations are relied upon almost exclusively in order to generate a logical interpretation of Copper Cliff’s alteration assemblages. An amalgamation of the per-hole petrography described in the previous chapter reveals the system to be somewhat different than the ideal representation of the porphyry system as put forth in Figures 2.6 and 2.7. The most conspicuous divergence is the presence of alunite over a vertical distance of over 1000 meters. In many instances, notably in hole 07DDCC004, alunite occurs as the dominant alteration mineral, and not as a weak remnant, even at lower elevations. Although alunite at high elevations is easily recognized as advanced argillic alteration (quartz + alunite + kaolinite ± dickite ± pyrophyllite), alunite at lower elevations cannot be classified as such. Alunite instead appears as part of the phyllic altered area, and the assemblage lacks the characteristics of the higher level advanced argillic alteration, such

as intense silicification and massive alunite. So, what appears to be a persistent overprint of advanced argillic by phyllic alteration at elevations below approximately 1000 meters ASL is in fact simply phyllic alteration with alunite. This indicates this was not an overprinting mineralizing event, but a further expression of the oxidation of the mineralizing fluid, since alunite is stable over such a large vertical extent. It is not until below approximately 500 meters, near to the deepest occurrences, that alunite is seen being replaced by white phylosilicates or smectite.

Deeper in the system, a far better example of alteration assemblage overprint is shown in the replacement of hydrothermal biotite (KSBC alteration) with white phyllosilicates and pyrite. This overprint is often incomplete, and is controlled by quartz veinlets with bleached selvages 1-2 centimeters in width. This is interpreted to show the final collapse of the system, as lower-temperature fluids from the cooling magma passed through potassic-altered rock on their way upwards to the epithermal environment (Heinrich et al. 2004).

### 4.3. Mineralization

Kennecott's exploration project has renewed hope that significant copper sulfide mineralization may exist below approximately 600 meters ASL (Figure 3.5), even though the current study has shown that the known system above this level is relatively sulfide-poor and sulfate-rich. This is especially true of the upper 1000 meters of the system between 1500 and 500 meters ASL, where alunite is most common and pyrite rarely peaks above 0.5%-volume. In this area, specular hematite is common as well. The prevalence of sulfate and the occurrence of hydrothermal hematite with pyrite indicate that the mineralizing fluids of the Copper Cliff system were iron-rich and oxidized, the latter of which has been shown to be a

common attribute of Cu-Au porphyries worldwide (Rowins 2000). Conditions for sulfide formation seem to improve below 500 meters with the more commonplace occurrence of chalcopyrite, bornite (an excellent gold host), and rare hypogene chalcocite replacing bornite. This increase can be seen in petrographic section as well as in assays, where copper and gold values increase. Recent sampling reveals phyllic-overprinted KSBC alteration to be the most heavily mineralized, in the form of Cu-sulfide-bearing quartz veinlets, as well as less common disseminations thereof. However, additional samples are required to fully characterize this deep region of the system, and were not available at the time of this study.

Three-dimensional block models constructed of the District's metal distributions offer comparison to the accepted porphyry model, as well as helping to delineate the core versus the outer limits of the known system. Zinc and lead (Figure 3.3) show concentration near the current topographic surface, although almost no lead or zinc sulfides were ever seen in drill core, and the base metal veins commonly found around large porphyry deposits are absent at Copper Cliff. Elevated values of gold and copper are present at the surface in the quartz-alunite district center, and are attributed to Cu-sulfosalts such as enargite, luzonite, and famatinite, with gold as microscopic inclusions of electrum mainly present in pyrite. Copper and gold are not seen in any significant concentration until below 500 meters ASL (Figure 3.4, 3.5), and the intervening zone is metal poor except for traces of copper as rare disseminated chalcopyrite. The increase below 500 meters ASL is shown in petrographic samples as the rise in copper-bearing sulfides below this elevation. Gold remains slightly below the porphyry average (0.2 g/t) even at low elevations, rarely rising above 0.15 g/t.

Interpretation of the distribution of gold at Copper Cliff, when combined with stable isotope data obtained from alunite and pyrite, offers further evidence concerning the system's

genesis. Porphyry-style ore deposits have long been recognized as major gold resources, although by tonnage the highest-grade concentrations of precious metals are restricted to their associated epithermal deposits (Muntean and Einaudi 2001). In the formation of precious metal-rich epithermal systems, the accepted model is that an $H_2S$-enriched vapor separates from saline magmatic brine at depth. Being more buoyant, this volatile phase rises, carrying metals, and interacts with meteoric waters to create an acidic hypogene fluid, which is responsible for the deposit's alteration and mineralization signatures (Simmons et al. 2005; Heinrich et al. 2004).

However, this model does not apply to Copper Cliff. As has been stated earlier, alteration mineralogy at the property confirms that the mineralizing fluid was highly oxidizing and Fe-rich. The coexistence of plentiful Fe-oxides and Fe-sulfides points to the fluid having an excess of iron over sulfur, at least initially. Precipitation of pyrite from this Fe-rich ore fluid during cooling would have resulted in a rapid depletion of sulfur, destabilizing bisulfide ligands which are essential to the transport of precious metals at low temperatures (Heinrich et al. 2004). Therefore, most gold would have precipitated in the deeper, higher-temperature parts of the Copper Cliff system, as transport to cooler, epithermal environments would have been rendered impossible. Ideally, the model of epithermal orebody formation in which a sulfur-rich vapor phase separates from the saline fluid at depth would preserve the stability of bisulfide ligands. The lack of precious metals in the shallow regions of the Copper Cliff system consequently supports emplacement by a single-phase fluid, from which a vapor phase was never separated (Heinrich et al. 2004).

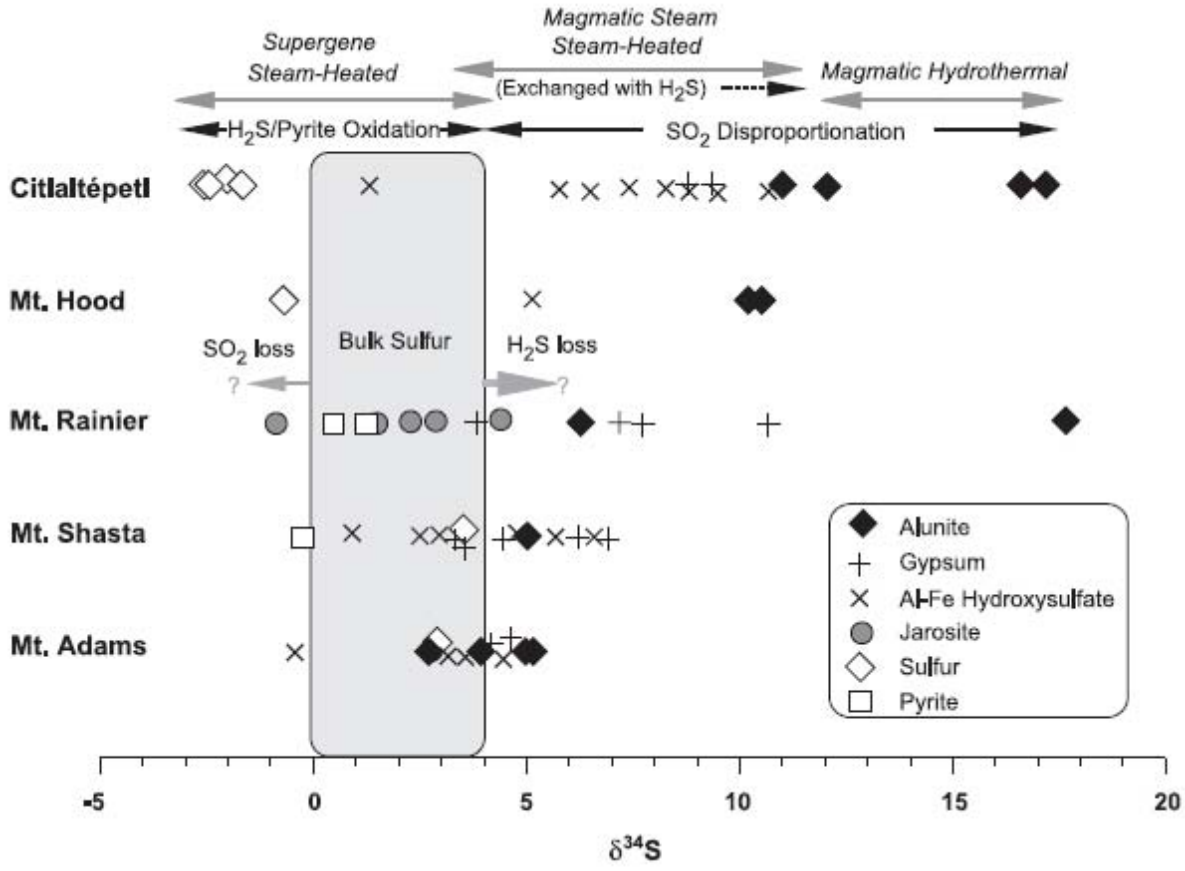


Figure 4.1. Graph from Rye (2005) showing $\delta^{34}S$ values for various minerals in active volcanic-hydrothermal systems. An average value of ~20‰ for Copper Cliff alunite correlates with a magmatic-hydrothermal origin.

Emplacement by a single-phase fluid at low temperature is substantiated by stable isotope values of sulfur in alunite and pyrite samples from the system. In a typical case of epithermal deposit formation, boiling of rising ore fluids will result in an $H_2S$-rich vapor, which interacts with meteoric water at high elevations within the system. Subsequent oxidation results in sulfuric acid, from which sulfate minerals such as alunite can precipitate. The $\delta^{34}S$ value of alunite that results from this chain of events will inherit the $\delta^{34}S$ value of the original $H_2S$-rich magmatic vapor. In most cases, this will be near 0‰, the same as the value of the original melt. However, as shown in Figure 3.15, these are not the $\delta^{34}S$ values

of alunite at Copper Cliff. Rather, we see a difference between sulfide and sulfate species of ~31‰, which suggests a near equilibrium fractionation between the two. This can only have resulted from the oxidation of an aqueous fluid, in which sulfate and sulfide held a close spatial relationship throughout the process. This would result in isotopically light $H_2S$ and heavy $H_2SO_4$, and minerals resulting from either would share the parent material's $\delta^{34}S$ value. This suggests that alunite at Copper Cliff was not formed in the customary epithermal style, but was rather emplaced directly by an oxidized, sulfate-rich, single-phase magmatic fluid (Rye 2005). In this situation, a substantial $H_2S$-rich vapor phase was not present.

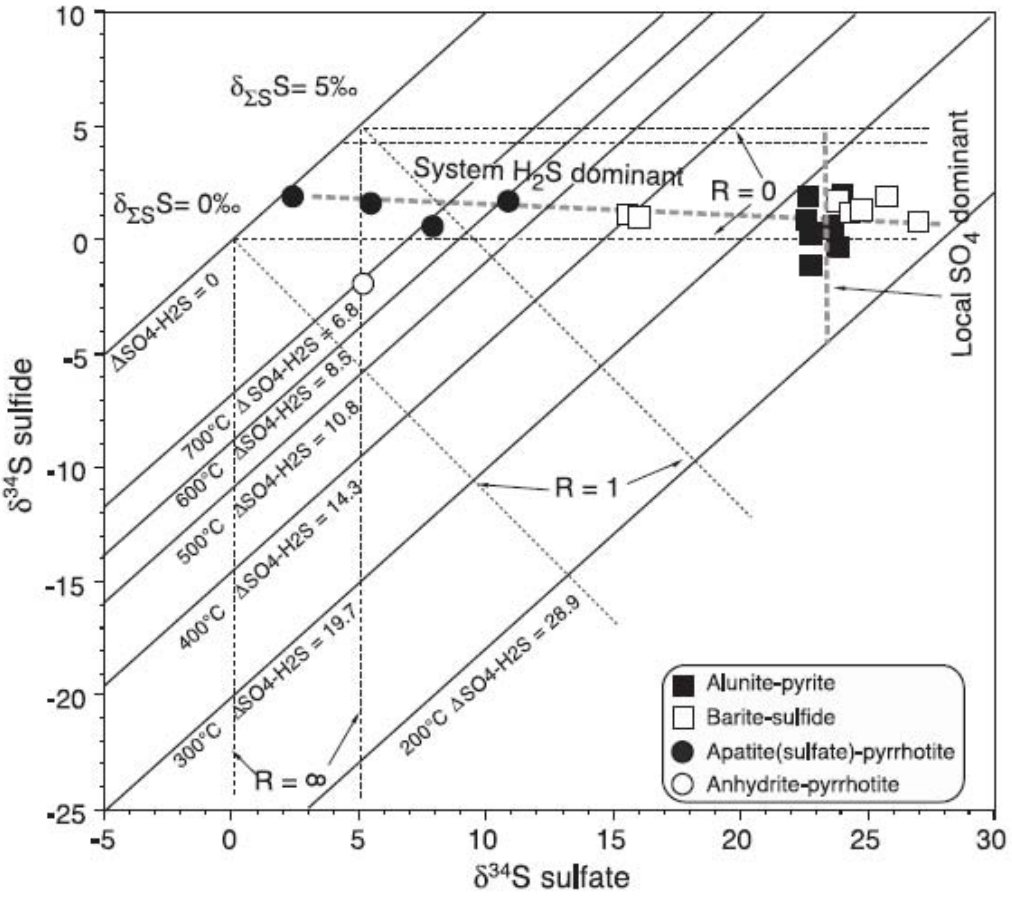


Figure 4.2. Rye's (2005) diagram relating temperature to fractionation between sulfide and sulfate species in hydrothermal systems. With sulfide at ~-11‰ and sulfate at ~+20‰, the Copper Cliff system is situated near the 200°C line.

Additional information is gained from the fractionation between sulfate and sulfide at Copper Cliff. Isotopic fractionation is higher at low temperatures than at high temperatures, and the calculated value of ~32‰ for $\Delta SO_4$-$H_2S$ suggests a low temperature during formation of alunite and pyrite in the system. Figure 4.2 reveals that fractionations of this level are associated with temperatures in the realm of 200°C, which is within the realm of epithermal temperatures.

# 5. CONCLUSIONS

The analysis options provided by the PIMA™ spectrometer and their applicability as an exploration tool is limited at Copper Cliff, based on this study. However, limitations of the instrument are not insurmountable, and it proved an invaluable tool for identifying and mapping important alteration minerals, especially alunite. With more careful sample selection and preparation it is possible that the PIMA™ could be used more effectively at this prospect to map a larger assortment of alteration assemblages, although the distinction between white phyllosilicate minerals of hydrothermal and metamorphic origin will remain problematic. As a vector to drilling, the SWIR spectroscopy has proven a powerful tool, along with traditional geology, geochemical sampling, and petrography. The PIMA™ was easily able to identify the quartz-alunite center of the district, and at Copper Cliff, a vertical hole drilled in this center encountered the highest copper and gold values of any other hole drilled at the prospect to date. This is not to say that this will be the case in every prospect, although it is a strong indicator of the potential of the instrument. In cases in which large areas must be sampled quickly and spatial resolution is not a primary concern, airborne techniques such as ASTER and AVIRIS hold distinct advantages over the PIMA™ for their

ability to gather immense amounts of information and delineate targets for the later, finer exploration techniques for which the PIMA™ is more suited.

Based on current sampling and analysis, Copper Cliff is a sulfide-poor, sulfate-rich porphyry system that has undergone extensive alteration during the course of a dynamic mineralizing event. Isotopic and petrographic work indicates that the parent ore fluid was oxidized and Fe-rich, and high-level mineralization took place at temperatures at or below 200°C. Quartz-alunite advanced argillic alteration is low in gold because the magmatic fluids interacted directly with meteoric waters, having likely risen along local structures, and precious metals were never significantly concentrated in or transported by bisulfide complexes to the epithermal environment due to single phase nature of the mineralizing fluid. However, these conclusions can only be applied to the system between 1500 and 800 meters. Drilling and sampling information below this level is incomplete, and petrographic analysis has shown that significant alteration and mineralization changes take place below 600 meters ASL, including decreases in alunite, and increases in copper- and gold-bearing sulfides. Additional work is necessary to fully characterize the Copper Cliff system from the highest epithermal to the lowest porphyry environments. However, this work has shown that the system, while not ideal, is intact and extensively developed, with potential for substantial mineralization at depth.

Figure 5.1 is a graphical representation of the known system's alteration and mineralization as described by this study (refer to Figure 3.7 for cross-section location). As shown in the section, while alunite is ubiquitous in most holes above approximately 750 meters ASL, it cannot be classified as advanced argillic, as it lacks other mineralogical characteristics. Besides having less alunite than higher level altered rocks, it lacks the

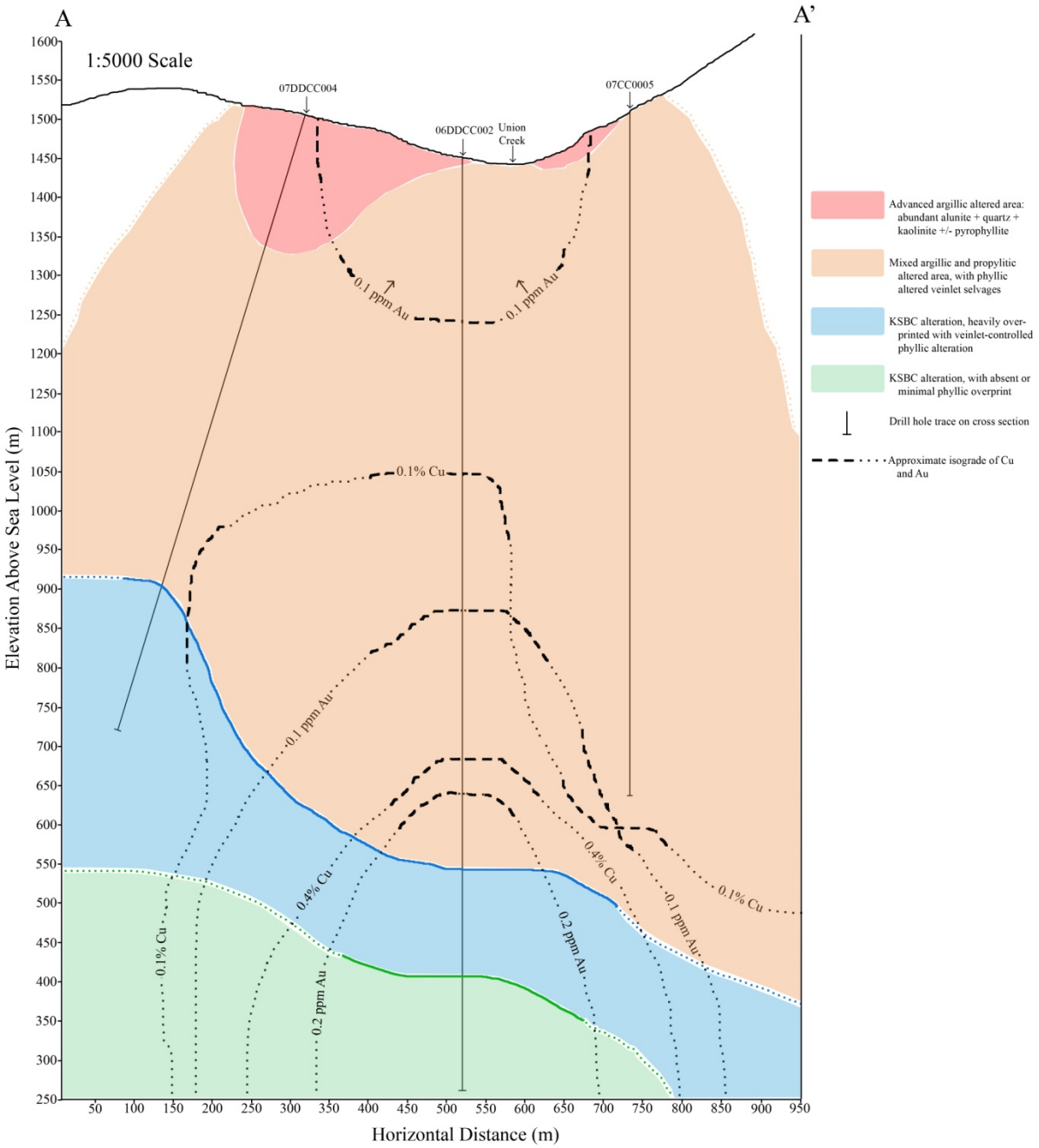


Figure 5.1. A cross-section of the known deposit, comprising the sum of petrographic, PIMA, assay, and isotopic data.

intense silicification and kaolinite of the advanced argillic altered areas. A large area of mixed argillic/intermediate argillic/propylitic alteration fills the intervening space between the advanced argillic altered area and the phyllic-overprinted KSBC alteration. This zone is characterized by low metal content (0.05-0.15%-wt Cu and 25-100 ppb Au) and <0.5%-vol pyrite, as well as frequent phyllic overprint along faults, fractures, and quartz-pyrite veinlet selvages. The aforementioned phyllic-overprinted KSBC altered area contains some of the best grades found in the district, with averages between 0.5 and 0.6%-wt Cu and 200 ppb Au. Hole 004 penetrated this altered area, but failed to encounter the significant mineralization found in hole 002. Hole 0005 was either not deep enough or is outside the main altered area, although it is impossible to tell given the current level of knowledge. However, based on this study it can be tentatively recommended that future drilling focus on what appears to be a deep, narrow zone of significant grade to the east of the Union Creek Fault. Holes collared to the east and northeast of hole 002 have the best chance of encountering further mineralization.

Investigations by Kennecott Exploration are ongoing at Copper Cliff as of 2009, and the potential for major discovery remains high, due to trends seen in the deepest section of the system, and this study's conclusions about the prospect are encouraging. Copper Cliff shares many characteristics of world-class Cu-Au porphyry deposits, as well as exhibiting other less common ones which may prove to be advantageous, such as the probable concentration of gold in the porphyry environment. Future exploration should focus on the footwall of the Union Creek Fault down to -500 meters ASL in order to fully delineate the system and begin to determine its structural fragmentation.

# BIBLIOGRAPHY


Arribas, A., Jr., Cunningham, C.G., Rytuba, J.J., Rye, R.O., Kelly, W.C., Podwysocki, M.H., McKee, E.H., and Tosdal. R.M., 1995, Geology, geochronology, fluid inclusions, and isotope geochemistry of the Rodalquilar gold-alunite deposit, Spain: Economic Geology, v. 90, p. 795-822.

Berger, B.R., King, T.V.V., Morath, L.C., and Phillips, J.D., 2003, Utility of High-Altitude Infrared Spectral Data in Mineral Exploration: Application to Northern Patagonia Mountains, Arizona: Economic Geology, v. 98, p. 1003-1018.

Bonham, H.F., Jr., 1988, Models for volcanic-hosted epithermal precious metal deposits, *in* Bulk minable precious metal deposits of the Western United States, Symposium Proceedings: Geologic Society of Nevada, 755 p.

Brannon, C.A., Crebs, T.J., Klem, R., Riese, W.C., 1982, Copper Cliff Annual Report, Missoula and Granite Counties, Montana: Anaconda Copper Company, internal report (unpublished),
18 p.

Carter, B.A., 1982, Geology of the Eocene volcanic sequence, Mt. Baldy-Union Peak area, central Garnet Range, Montana [unpublished MS thesis]: University of Montana, Missoula, 55 p.

Childs, J.F., and Mulholland, P.S., 1988, Summary report on the Copper Cliff copper/gold submittal: Pegasus Corp. In-house report [unpublished], 19 p.

Cox, B., Gignoux, T., and McCulloch, 1998, Economic geology in the western portion of the Blackfoot River region; Discussion and Field Trip Guide: Northwest Geology, Vol. 28, pp. 101-109.

Duba, D. and Williams-Jones, A., 1983, The application of illite crystallinity, organic matter reflectance, and isotopic techniques to mineral exploration: A case study in southwestern Gaspe, Quebec: Economic Geology, v. 78, p. 1350-1363.

Earll, F.N., 1963, Economic Geology and Metallic Resources [of the Garnet Range], *in* Kauffman, M.E., Geology of the Garnet-Bearmouth Area, Western Montana: Montana Bureau of Mines and Geology, Butte, Montana, Memoir 39.

Ellsworth, P.C., 1993, Alteration and Mineralization of the Copper Cliff Prospect, Garnet Range, Montana: University of Montana, unpublished master's thesis, 62 p.

Harrison, J.E., Griggs, A.B., and Wells, J.D., 1974, Tectonic features of the Precambrian Belt basin and their influence on post-belt structures: USGS Professional Paper 866.

Hawe, R.G., 1974, A Combined Magnetic Resistivity and Geochemist Exploration Study of the Copper Cliff Mining District: unpublished report by independent geophysical contractor, 30 p.

Hedenquist, J.W., Arribas, A., Jr., and Reynolds, T.J., 1998, Evolution of an intrusion-centered hydrothermal system: Far Southeast-Lepanto porphyry and epithermal Cu-Au deposits, Phillipines: Economic Geology, v.93, p. 373-404.

Heinrich, C.A., Driesner, T., Stefánsson, A., and Seward, T.M., 2004, Magmatic vapor contraction and the transport of gold from the porphyry environment to epithermal ore deposits: Geology, v. 32, no. 9, p. 761-764.

Irving, J.G., 1963, Report on the Copper Cliff mining district, Missoula and Granite Counties, Montana: Inhouse Consultant Report to the American Mining Company, 54 p.

James, A.H., 1971, Hypothetical diagram of several porphyry copper deposits: Economic Geology, v. 66, p. 43-47.

Jin, Z., Zhu, J., Ji, J.,Li, F., and Lu, X., 2002, Two origins of illite at the Dexing porphyry Cu deposits, East China: Implications for ore-forming fluid constraints on illite crystallinity: Clays and Clay Minerals, v. 50, p. 381-400.

Johnson, J.J., 1972, Report on sampling and analysis of the Copper Cliff outcrop, Copper Cliff district, Missoula County, Montana: Unpublished report, 8 p.

Kauffman, M.E., 1963, Geology of the Garnet-Bearthmouth Area, Western Montana: Montana Bureau of Mines and Geology, Memoir 39, 40 p.

Lowell, J.D. and Guilbert, J.M., 1970, Lateral and vertical alteration-mineralization zoning in porphyry ore deposits: Economic Geology, v. 65, p. 373-408.

Mann, L., and Sears, J., 2004, The contact metamorphic aureole of the late Cretaceous Gamet Stock, Garnet-Coloma area, Montana: Northwest Geology, vol. 33, pp. 34-48.

Mars, J.C. and Rowan, L.C., 2006, Regional mapping of phyllic- and argillic-altered rocks in

the Zagros magmatic arc, Iran, using Advanced Spaceborne Thermal Emission and Reflection Radiometer (ASTER) data and logical operator algorithms: Geosphere, v. 2, no. 3, p. 161-187.

Martinez, A.S.E., Goetz, A.F.H., Atkinson, Jr., W.W., Kruse, F.A., Eberl, D.D., 1999, Multiscale study of infrared spectra of clay minerals: from *ab initio* quantum calculations to hyperspectral remote sensing: Proceedings of the Thematic Conference on Geologic Remote Sensing, v. 13, no. 1, p. 174-181.

Muntean, J.L. and Einaudi, M.T., 2001, Porphyry-Epithermal Transition: Maricunga Belt, Northern Chile: Economic Geology, v. 96, p. 743-772.

Pardee, J.T., 1917, Ore deposits of the northwestern part of the Garnet Range, MT: Geological Survey Bulletin 660-F, contributions to economic geology, pt. 1.

Parry, W., Jasumback, M., and Wilson, P., 2002, Clay mineralogy of phyllic and intermediate argillic alteration at Bingham, Utah: Economic Geology, v.97, p. 221-239

Pederson, R. J., 1988, Preliminary evaluation report on the Copper Cliff and Garnet prospects, Missoula and Granite Counties, Montana: Western Energy Company unpublished in-house report, 29 p.

Reynolds, M.W., 1979, Character and extent of basin-range faulting, western Montana and east-central Idaho, *in* Newman, G.W. and Goode, H.D., (eds.), Basin and Range Symposium: Rocky Mountain Association of Geologists and Utah Geological Association, p. 185-193.

Reynolds, P.H., 1991, Structural geology of the Blackfoot Thrust system in the Cramer Creek area, Missoula County, Montana [unpublished MSc thesis]: University of Montana, Missoula, 70 p.

Rose, A.W., 1970, Zonal relations of wallrock alteration and sulfide distribution at porphyry copper deposits: Economic Geology, v. 65, p. 920-936.

Rowins, Stephen M., 2000, Reduced porphyry copper-gold deposits: A new variation on an old theme: Geology, v. 28, no.6, p.491-494.

Rye, R.O., 1993, The evolution of magmatic fluids in the epithermal environment: The stable isotope perspective: Economic Geology, v. 88, p. 733-752.

Rye, R.O., 2005, A review of the stable-isotope geochemistry of sulfate minerals in selected igneous environments and related hydrothermal systems: Chemical Geology, v. 215, p. 5-36.

Rye, R.O., Bethke, P.M ., and Wasserman, M.D., 1992, The stable isotope geochemistry of acid sulfate alteration: Economic Geology, v. 87, p. 225-262.

Sahinen, U.M., 1957, Mines and mineral deposits, Missoula and Ravalli Counties, Montana: Montana Bureau of Mines and Geology Bull. 8, p. 28-31.

Sears, J.W., Weiss, C.P., Reynolds, P.H., and Griffin, J.H., 1989, A structural section through a 25-km thick thrust plate in west-central Montana: a field trip from Paradise to Garrison, *in* Chamberlain, V.E., Breckenridge, R.M., and Bonnichsen, B., (eds.), Guidebook to the geology of northern and western Idaho and surrounding area: Idaho Geological Survey Bulletin 28, p. 87-102.

Seedorf, E., Dilles, J.H., Proffett, Jr., J.M., Einaudi, M.T., Zurcher, L., Stavast, W.J.A., Johnson, D.A., and Barton, M.D., 2005, Porphyry Deposits: Characteristics and Origin of Hypogene Features, *in* Economic Geology 100th Anniversary Volume, pp. 251-298.

Sillitoe, R.H., 1973, The tops and bottoms of porphyry copper deposits: Economic Geology, v. 68, p. 799-815.

Sillitoe, R.H., 1983, Enargite-bearing massive sulfide deposits high in porphyry copper systems: Economic Geology, v. 78, p. 348-352.

Sillitoe, R.B., 1988, Gold and silver deposits in porphyry systems, *in* Shafer, R.. W., Cooper, J.J., and Vikre, P.G., eds., Bulk minable precious metal deposits of the western United States, Symposium Proceedings: Reno, Geologic Society of Nevada, p. 233-257.

Sillitoe, R.H., 1995, Exploration of porphyry copper lithocaps: Australasian Institute of Mining and Metallurgy Publication Series 9/95, p. 527-532.

Simmons, S.F., White, N.C., and John, D.A., 2005, Geological Characteristics of Epithermal Precious and Base Metal Deposits, *in* Economic Geology 100th Anniversary Volume: Society of Economic Geologists, Inc., pp. 485-522.

Verdel, C.S., Knepper, Jr., D., Livo, K.E., McLemore, V.T., Penn, B., Keller, R., 2000, Mapping Minerals at the Copper Flat Porphyry, New Mexico, Using AVIRIS Data: Proceedings of the 10th JPL Airborne Earth Science Workshop, JPL Publication, p. 427-433.

Vice, D.H, 1989, The mineral resource potential of the Garnet Range, west-central Montana *in* French, D.E. and Grabb, R.E., (eds.), Montana Geologic Society 1989 field conference guidebook, Montana centennial edition: Geologic resource, v. 1. Field-Conference-Montana-Geologic-Society, p. 411-414.

Weed, W.H. and Gow, P.A., Geologic report on property of Potomac Copper Company: Unpublished report, 16 p.

Wallace, A.B., 1979, Possible signatures of buried porphyry-copper deposits in middle to late Tertiary volcanic rocks of western Nevada: Nevada Bureau of Mines Report 33, p. 69-75.

Wallace, C.A., Kleeper, M.R., and Scarborough, D.M., 1977, Preliminary Reconnaissance Geologic Maps of the Garnet Range, Western Montana: USGS Open File Report 77-529.

Yang, K., Lian, C., Huntington, J.F., Peng, Q., and Wang, Q., 2005, Infrared spectral reflectance characterization of the hydrothermal alteration at the Tuwu Cu-Au deposit, Xinjiang, China: Mineralium Deposita, v. 40, p. 324-336.

# APPENDIX – TABULATED PETROGRAPHIC DATA

| | | PIMA Readings | | | | Opaque Minerals | | | | |
|---|---|---|---|---|---|---|---|---|---|---|
| Drill Hole | Elevation ASL (m) | Min 1 | Min 2 | Min 3 | Min 4 | Min 1 | Min 2 | Min 3 | Min 4 | Min 5 |
| 07DDCC004 | 1479.99 | K_Alunite | * | * | * | * | * | * | * | * |
| 07DDCC004 | 1457.42 | Halloysite | Muscovite | * | * | py | cpy | cc | born | * |
| 07DDCC004 | 1398.96 | K_Alunite | * | * | * | * | * | * | * | * |
| 07DDCC004 | 1367.30 | * | * | * | * | py | * | * | * | * |
| 07DDCC004 | 1293.13 | * | * | * | * | py | * | * | * | * |
| 07DDCC004 | 1256.00 | * | * | * | * | py | * | * | * | * |
| 07DDCC004 | 1205.88 | K_Alunite | Pyrophillite | Na_Alunite | * | py | * | * | * | * |
| 07DDCC004 | 1165.01 | Dickite | Halloysite | K_Alunite | * | py | * | * | * | * |
| 07DDCC004 | 1108.85 | Muscovite | Halloysite | Paragonite | * | py | mo | cpy | * | * |
| 07DDCC004 | 1073.30 | * | * | * | * | py | * | * | * | * |
| 07DDCC004 | 1031.00 | Halloysite | Muscovite | * | * | py | * | * | * | * |
| 07DDCC004 | 1022.20 | * | * | * | * | py | * | * | * | * |
| 07DDCC004 | 1005.81 | Kaolinite | K_Alunite | * | * | py | mo | ssalts | * | * |
| 07DDCC004 | 963.65 | Kaolinite | Phlogopite2 | * | * | * | * | * | * | * |
| 07DDCC004 | 941.62 | * | * | * | * | py | mo | * | * | * |
| 07DDCC004 | 909.00 | * | * | * | * | py | mo | * | * | * |
| 07DDCC004 | 902.35 | Illite | Kaolinite | Halloysite | Montmorillonite | py | | * | * | * |
| 07DDCC004 | 727.43 | * | * | * | * | py | mo | mag | * | * |
| 06DDCC002 | 736.30 | * | * | * | * | py | * | * | * | * |
| 06DDCC003 | 691.10 | * | * | * | * | py | cpy | * | * | * |
| 06DDCC004 | 644.70 | * | * | * | * | py | hem | cpy | born | * |
| 06DDCC005 | 602.60 | * | * | * | * | py | cpy | hem | * | * |
| 06DDCC006 | 599.60 | * | * | * | * | py | cpy | * | * | * |
| 06DDCC002 | 472.24 | Kaolinite | Paragonite | * | * | py | cpy | born | cc | mo |
| 06DDCC002 | 415.06 | Kaolinite | Pyrophillite | * | * | py | cpy | born | cc | * |
| 06DDCC002 | 414.54 | Kaolinite | * | * | * | py | * | * | * | * |
| 06DDCC002 | 407.93 | * | * | * | * | py | cpy | mo | * | * |
| 06DDCC002 | 407.47 | Illite | Kaolinite | Muscovite | Pyrophillite | py | born | cc | * | * |
| 06DDCC002 | 387.36 | * | * | * | * | py | mo | hem | * | * |
| 06DDCC002 | 387.36 | * | * | * | * | py | mo | * | * | * |
| 06DDCC002 | 353.57 | Kaolinite | Muscovite | Paragonite | Pyrophillite | py | hem | * | * | * |
| 06DDCC002 | 278.49 | Kaolinite | Muscovite | * | * | py | * | * | * | * |
| 07DDCC003 | 1488.68 | * | * | * | * | mag | hem | * | * | * |
| 07DDCC003 | 1299.90 | * | * | * | * | py | mag | * | * | * |
| 07DDCC003 | 1244.40 | K_Alunite | Na_Alunite | Kaolinite | * | py | mo | * | * | * |
| 07DDCC003 | 1211.56 | Pyrophillite | Paragonite | K_Alunite | * | py | mo | cpy | * | * |
| 07DDCC003 | 1081.81 | K_Alunite | Illite | Kaolinite | Pyrophillite | py | mo | cpy | * | * |
| 07DDCC003 | 1060.23 | Illite | * | * | * | hem | py | mag | cpy | * |
| 07DDCC003 | 1027.80 | * | * | * | * | py | * | * | * | * |
| 07DDCC003 | 975.16 | Illite | * | * | * | py | mo | hem | * | * |
| 07DDCC003 | 918.50 | Illite | Kaolinite | Muscovite | * | py | * | * | * | * |
| 07CC005 | 1458.24 | Illite | Kaolinite | * | * | py | mag | hem | * | * |
| 07CC005 | 1424.54 | * | * | * | * | mag | * | * | * | * |
| 07CC005 | 1376.68 | Illite | * | * | * | py | mag | hem | * | * |
| 07CC005 | 1188.15 | Muscovite | Paragonite | * | * | py | hem | cpy | * | * |
| 07CC005 | 1162.04 | * | * | * | * | hem | py | * | * | * |
| 07CC005 | 1106.48 | Illite | Calcite | * | * | py | mo | hem | * | * |
| 07CC005 | 1097.56 | Illite | * | * | * | py | cpy | * | * | * |
| 07CC005 | 1080.60 | Illite | MgChlorite | * | * | py | * | * | * | * |
| 07CC005 | 1033.14 | * | * | * | * | hem | cpy | py | * | * |
| 07CC005 | 999.59 | Illite | * | * | * | py | cpy | hem | * | * |
| 07CC005 | 991.50 | IntChlorite | Illite | * | * | py | cpy | hem | * | * |
| 07CC005 | 956.07 | * | * | * | * | hem | py | cpy | * | * |
| 07CC005 | 948.10 | * | * | * | * | mag | hem | cpy | py | * |
| 07CC005 | 930.40 | * | * | * | * | mag | hem | cpy | * | * |

| Alteration Minerals | | | | | | | | Primary Minerals | | | | | Alteration | | |
|---|---|---|---|---|---|---|---|---|---|---|---|---|---|---|---|
| Min 1 | Min 2 | Min 3 | Min 4 | Min 5 | Min 6 | Min 7 | Min 8 | Min 1 | Min 2 | Min 3 | Min 4 | Protolith | Primary | Overprint 1 | Overprint 2 |
| qtz | alun | kaol | * | * | * | * | * | * | * | * | * | undeterminable | Adv argillic | silicification | * |
| qtz | wp | halloy | carb | * | * | * | * | * | * | * | * | latite porphyry | Phyllic | silicification | * |
| qtz | alun | * | * | * | * | * | * | * | * | * | * | latite porphyry | Adv argillic | * | * |
| qtz | kaol | smct | alun | * | * | * | * | * | * | * | * | latite porphyry | Adv argillic | Vuggy silica | * |
| bio | qtz | kaol | chlor | jaro | * | * | * | bio | amph | * | * | latite porphyry | K-silicate bio-construct | Int argillic | * |
| qtz | kaol | alun | wp | * | * | * | * | * | * | * | * | latite porphyry | Adv argillic | Vuggy silica | * |
| qtz | alun | pyro | kaol | * | * | * | * | * | * | * | * | latite porphyry | Adv argillic | * | * |
| qtz | alun | dick | halloy | * | * | * | * | * | * | * | * | latite porphyry | Adv argillic | * | * |
| wp | qtz | alun | halloy | * | * | * | * | bio | * | * | * | latite porphyry | Adv argillic | phyllic | * |
| qtz | alun | kaol | wp | * | * | * | * | * | * | * | * | latite porphyry | Adv argillic | phyllic | * |
| qtz | wp | halloy | bio | * | * | * | * | bio | * | * | * | latite porphyry | Phyllic | K-silicate bio-construct | * |
| qtz | wp | alun | kaol | * | * | * | * | * | * | * | * | latite porphyry | Adv argillic | phyllic | * |
| alun | kaol | qtz | * | * | * | * | * | * | * | * | * | undeterminable | Adv argillic | * | * |
| qtz | kaol | wp | * | * | * | * | * | bio | * | * | * | latite porphyry | Sericitization | * | * |
| qtz | wp | kaol | * | * | * | * | * | * | * | * | * | quartzite | Phyllic | * | * |
| qtz | pyro | alun | kaol | * | * | * | * | * | * | * | * | undeterminable | Adv argillic | * | * |
| bio | smct | qtz | wp | kaol | * | * | * | bio | amph | qtz | * | latite porphyry | K-silicate bio-construct | phyllic | * |
| bio | smct | qtz | chlor | carb | kspar | wp | amph | bio | amph | qtz | * | latite porphyry | K-silicate bio-construct | carbonate | phyllic |
| qtz | wp | * | * | * | * | * | * | bio | * | * | * | latite porphyry | Phyllic | * | * |
| qtz | wp | bio | * | * | * | * | * | bio | * | * | * | latite porphyry | K-silicate bio-construct | phyllic | * |
| qtz | wp | smct | chlor | * | * | * | * | * | * | * | * | quartzite | Phyllic | Int argillic | * |
| qtz | * | * | * | * | * | * | * | * | * | * | * | undeterminable | * | * | * |
| qtz | wp | alun | kaol | * | * | * | * | * | * | * | * | undeterminable | Phyllic | silicification | Adv argillic |
| qtz | wp | alun | kaol | epid | * | * | * | * | * | * | * | quartzite | Phyllic | silicification | * |
| qtz | wp | smct | kaol | pyro | * | * | * | * | * | * | * | quartzite | Int argillic | phyllic | * |
| qtz | wp | kaol | smct | * | * | * | * | * | * | * | * | quartzite | Phyllic | * | * |
| qtz | bio | wp | * | * | * | * | * | bio | * | * | * | latite porphyry | K-silicate bio-construct | phyllic | * |
| qtz | wp | kaol | dick | pyro | * | * | * | * | * | * | * | quartzite | Int argillic | phyllic | * |
| qtz | wp | bio | * | * | * | * | * | bio | * | * | * | latite porphyry | K-silicate bio-construct | phyllic | * |
| bio | qtz | wp | * | * | * | * | * | bio | * | * | * | latite porphyry | K-silicate bio-construct | phyllic | * |
| qtz | wp | kaol | tour | smct | * | * | * | * | * | * | * | quartzite | Int argillic | phyllic | * |
| qtz | wp | bio | carb | * | * | * | * | bio | * | * | * | latite porphyry | K-silicate bio-construct | phyllic | * |
| qtz | smct | kaol | wp | * | * | * | * | qtz | plag | bio | kspar | latite porphyry | Int argillic | * | * |
| qtz | alun | * | * | * | * | * | * | * | * | * | * | undeterminable | Adv argillic | * | * |
| qtz | alun | * | * | * | * | * | * | * | * | * | * | latite porphyry | Adv argillic | * | * |
| qtz | wp | kaol | pyro | alun | * | * | * | * | * | * | * | undeterminable | Adv argillic | phyllic | * |
| qtz | alun | kaol | wp | * | * | * | * | * | * | * | * | quartzite | Adv argillic | phyllic | * |
| qtz | kaol | wp | smct | carb | * | * | * | * | * | * | * | latite porphyry | Int argillic | phyllic | Carbonate |
| qtz | wp | kaol | diasp | alun | carb | * | * | * | * | * | * | quartzite | Adv argillic | phyllic | * |
| qtz | carb | kaol | wp | * | * | * | * | * | * | * | * | quartzite | Carbonate | phyllic | * |
| qtz | kaol | wp | * | * | * | * | * | * | * | * | * | quartzite | Phyllic | * | * |
| qtz | kaol | chlor | wp | * | * | * | * | amph | * | * | * | latite porphyry | Phyllic | * | * |
| carb | grnt | pyrx | qtz | amph | * | * | * | amph | * | * | * | latite porphyry | Skarn | * | * |
| qtz | wp | carb | halloy | * | * | * | * | * | * | * | * | undeterminable | Phyllic | * | * |
| qtz | wp | kaol | * | * | * | * | * | amph | * | * | * | latite porphyry | Phyllic | * | * |
| qtz | wp | epid | * | * | * | * | * | amph | * | * | * | latite porphyry | Phyllic | * | * |
| qtz | carb | wp | kaol | alun | * | * | * | * | * | * | * | latite porphyry | Adv argillic | carbonate | phyllic |
| qtz | kaol | smct | wp | carb | halloy | * | * | amph | bio | * | * | latite porphyry | Adv argillic | phyllic | * |
| qtz | wp | kaol | carb | * | * | * | * | amph | * | * | * | latite porphyry | Phyllic | carbonate | * |
| qtz | kaol | wp | * | * | * | * | * | amph | * | * | * | latite porphyry | Phyllic | * | * |
| qtz | wp | kaol | * | * | * | * | * | * | * | * | * | undeterminable | Phyllic | * | * |
| qtz | kaol | wp | chlor | * | * | * | * | amph | * | * | * | latite porphyry | Phyllic | silicification | * |
| qtz | wp | smct | kaol | epid | * | * | * | * | * | * | * | quartzite | Adv argillic | phyllic | * |
| qtz | wp | epid | kaol | halloy | alun | * | * | * | * | * | * | quartzite | Adv argillic | phyllic | * |
| carb | kaol | dick | qtz | * | * | * | * | * | * | * | * | latite porphyry | Adv argillic | * | * |

| Comments |
| --- |
| silicified w/ heavy alunite component. |
| highly silicified w/ clay components. Cu minerals extremely uncommon!! |
| highly silicified adv argillic alt |
| sample divided in two b/w vuggy silica and adv argillic |
| potassic alt remnant w/ weak int argillic overprint |
| half n' half vuggy silica and adv argillic alt. |
| highly silicified |
| low temperature |
| very strong overprint of adv argillic by phyllic |
| very weak overprint by phyllic |
| appears to be bio-construct alt w/ strong phyllic overprint |
| Weak overprint |
| Extreme alteration. Pink sample of massv alunite vn. |
| Weakly altered. |
| 90% qtz. Relict textures destroyed. Qtz groundmass equigranular and euhedral. |
| 80% qtz. Relict textures destroyed completely. Mo + py on edge of offset, x-cutting qtz vn. |
| shreddy bio rplcing almost all primary min. bio-construct alt has smectite component; phyllic has kaolinite component |
| Vn x-cuts sample. Kspar halo, followed by carb halo and qtz core w/ sulfides. Bio-construct alteration strong and pervasive over all of sample. |
| weak pyrite component. |
| biotite constructive overprinted by phyllic. Trace Cu. Hydrothermal biotite being replaced by WP. |
| moderate phyllic with intermediate argillic overprint. No magmatic remnants visible. Trace Cu only. |
| Polished section only; no alteration petrography possible. Mineralized qtz veinlets. |
| weak evidence of advanced argillic alteration, overprinted by heavy silicification and phyllic alteration. ~0.5% Cu. |
| silicified phyllic alt |
| very weak presence of int argillic alt |
| classic QSP/phyllic alt. |
| potassic w/ strong phyllic overprint |
| int argillic with strong phyllic overprint and late-stage Cu-bearing sulfide stringer vns |
| trace mo + hem in x-cutting vnlet |
| many zircons in sample |
| intermediate argillic alt, strongly overprinted with phyllic. Alunite replaced w/ smectite; wp covers all. |
| half n' half potassic and potassic w/ phyllic overprint |
| extremely weak int argillic, with mag replacing hem |
| strong phyllic overprint of weak adv argillic |
| very weak overprint by phyllic |
| intense combination of two alteration types |
| Carbonate-flooded w/ weak phyllic characteristics |
| phyllic alt w/ kaol |
| strong carbonate alt w/ large areas completely flooded. Adv argillic weak, with phyllic being the next most prevalent alteration. |
| weak adv argillic w/ stronger phyllic overprint |
| phyllic alt w/ kaol and carb components |
| strong phyllic alt w/ kaol |
| strong phyllic alt w/ kaol |
| strong phyllic alt w/ kaol and silica |
| strong phyllic overprint of weak adv argillic |
| weak adv argillic w/ stronger phyllic overprint. Mag replacing hem. |
| weak adv argillic, w/ mag replacing hem |